Journal of Medicinal Chemistry

Design, (Radio)Synthesis, *in Vitro* and *in Vivo* Evaluation of highly selective and potent Matrix Metalloproteinase (MMP-12) Inhibitors as Radiotracers for Positron Emission Tomography

Viktoria Butsch, Frederik Börgel, Fabian Galla, Katrin Schwegmann, Sven Hermann, Michael Schäfers, Burkhard Riemann, Bernhard Wünsch, and Stefan Wagner

J. Med. Chem., **Just Accepted Manuscript** • DOI: 10.1021/acs.jmedchem.8b00200 • Publication Date (Web): 16 Apr 2018

Design, (Radio)Synthesis, *in Vitro* and *in Vivo* Evaluation of highly selective and potent Matrix Metalloproteinase 12 (MMP-12) Inhibitors as Radiotracers for Positron Emission Tomography

Viktoria Butsch,[a] Frederik Börgel,[b] Fabian Galla,[b] Katrin Schwegmann,[c] Sven Hermann,[c] Michael Schäfers, [a,c,d] Burkhard Riemann, [a] Bernhard Wünsch,[b,d,#] and Stefan Wagner [a,#,*]

[a]Department of Nuclear Medicine, University Hospital Münster, Albert-Schweitzer-Campus 1, Building A1, 48149 Münster, Germany

[b]Institute of Pharmaceutical and Medicinal Chemistry, University of Münster, Corrensstr. 48, 48149 Münster, Germany

[c]European Institute for Molecular Imaging, University of Münster, Waldeyerstraße 15, 48149 Münster, Germany

[d]Cells-in-Motion Cluster of Excellence (EXC 1003 – CiM), Westfälische Wilhelms-Universität Münster, Germany

[#] Both authors contributed equally to this work and share senior authorship

ABSTRACT

Dysregulated levels of activated matrix metalloproteinases (MMPs) are linked to different pathologies such as cancer, atherosclerosis, neuroinflammation and arthritis. Therefore imaging of MMPs with positron emission tomography (PET) represents a powerful tool for the diagnosis of MMP associated diseases. Moreover, to distinguish between the distinct functions and roles of individual MMPs in particular pathophysiological processes their specific imaging must be realized with radiolabeled tracers e.g. fluorine-18 labeled MMP inhibitors (MMPIs). Therefore, fluorinated dibenzofuransulfonamide-based MMPIs showing excellent inhibition of MMP-12 and selectivity over other MMPs were prepared. MMP-12 is a key enzyme in e.g. chronic obstructive pulmonary disease (COPD) and atherosclerosis. Due to promising *in vitro* properties, three candidates (**4**, **9** and **19**) were selected from this library and the radiofluorinated analogs (**[^{18}F]4**, **[^{18}F]9** and **[^{18}F]19**) were successfully synthesised. Initial *in vitro* serum stability and *in vivo* biodistribution studies of the radiolabeled MMPIs with PET demonstrated their potential benefit for preferable MMP-12 imaging.

INTRODUCTION

Matrixins also known as matrix metalloproteinases (MMPs) belong to the metzincin superfamily of proteases that also include serralysins, adamalysins, pappalysins and astacins. The MMP protease family consists of at least 23 members in vertebrates and shows proteolytic activity towards extracellular matrix (ECM) components (collagen, gelatin, elastin, laminin etc.) as well as non-matrix proteins (cytokines, chemokines, growth factors etc.).

Structurally MMPs are Ca^{2+}-containing endopeptidases with a Zn^{2+}-ion in the active site that is coordinated by three histidine-residues located in the highly conserved HEXGHXXGXXH

Zn^{2+}-binding motif.[1] MMPs play an important role in physiological processes such as organ morphogenesis, angiogenesis, wound healing and embryonic development.[2] Alongside activated MMPs are upregulated in many pathological processes[3] such as cancer,[4,5] atherosclerosis,[6,7] neuroinflammation,[8] arthritis[9] and pulmonary emphysema.[10] From this point of view MMPs represent highly (pre)clinical relevant and important targets for molecular imaging, e.g. with the nuclear medicine techniques single photon emission computed tomography (SPECT) and positron emission tomography (PET). Identification and diagnosis of tissues with upregulated levels of activated MMPs with SPECT and PET, respectively, would be a powerful instrument for the research of disorders involving MMPs as well as for the therapy of MMP associated diseases. Hence MMP inhibitors (MMPIs) labeled with SPECT-compatible nuclides (^{99m}Tc, ^{111}In, ^{123}I etc.) and radioisotopes suitable for PET (^{18}F, ^{11}C, ^{68}Ga, ^{124}I etc.), respectively, might be an appropriate tool for MMP imaging in nuclear medicine.[11]

Therefore our group focused on the development of small molecule radiolabeled MMPIs with broad spectrum inhibition profile based on the lead structures (*R*)-*N*-hydroxy-2-((4-methoxy-*N*-(pyridin-3-ylmethyl)phenyl)sulfonamido)-3-methylbutanamide (CGS 27023A, Figure 1)[12] and (*R*)-2-((*N*-benzyl-4-methoxyphenyl)sulfonamido)-*N*-hydroxy-3-methylbutanamide (CGS 25966).[13] We developed SPECT- and PET- compatible MMPIs of several generations that coordinate the Zn^{2+}-ion of the active site with a hydroxamate moiety. The MMPIs of the first generation contained iodine-123 (HO-[^{123}I]I-CGS 27023A) and facilitated imaging of MMP activity in the arterial wall in mice *in vivo*,[14,15] while representatives of the second generation incorporated fluorine-18[16,17,18] and the PET-tracer [^{18}F]BR351 out of this pool provided a sensitive, noninvasive diagnostic tool of following lesion formation and resolution in murine experimental autoimmune encephalomyelitis (EAE) and human multiple sclerosis (MS).[19,20] The

third generation, also labeled with fluorine-18, was modified with hydrophilic structural elements (e.g. 1,2,3-triazol ring(s), ethylene glycol units) resulting in a triazol-substituted candidate ([^{18}F]HUG38) that lent itself for further (pre)clinical evaluation.[21,22,23]

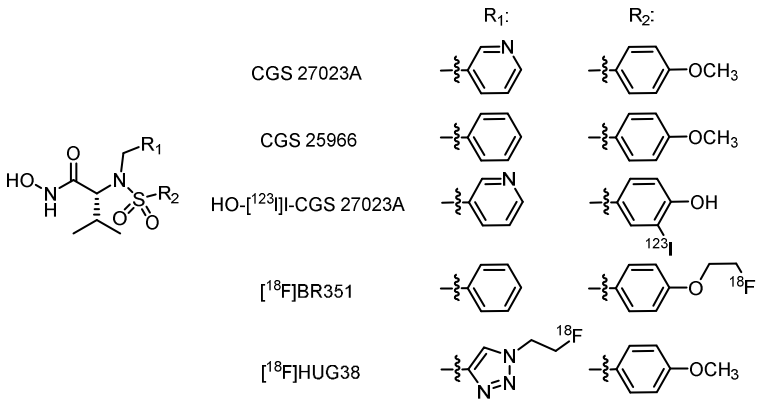

Figure 1. Hydroxamate based MMPIs CGS 27023A and CGS 25966 and radiolabeled derivatives.

Moreover barbiturate (pyrimidine-2,4,6-trione) based MMPIs that showed subgroup-specificity for the gelatinases A and B (MMP-2 and -9), neutrophil collagenase (MMP-8) and the membrane-bound MMPs MT-1-MMP (MMP-14) and MT-3-MMP (MMP-16)[24] were developed as radiotracers in our group. These compounds can also be subdivided in several classes (class 1: ^{123}I- , ^{124}I- and ^{125}I-labeled[25,26]; class 2: ^{18}F-labeled[27]; class 3: ^{18}F-labeled with hydrophilic structural modifications[28]). The prototype of ^{18}F-labeled barbiturates (class 2) was systematically evaluated in a colorectal cancer model but turned out to be not useful for MMP-9 imaging in this mouse model.[29] Furthermore in cooperation with other groups we developed ^{18}F-labeled prolin based[30] and ^{11}C-/^{18}F- and ^{68}Ga-labeled pyrimidine dicarboxamide based MMPIs[31] specific for collagenase-3 (MMP-13), a major proteolytic enzyme in ECM breakdown of osteoarthritis (OA) and rheumatoid arthritis (RA).[32]

In this project we aim at the development of MMPI radiotracers that are potent and selective for macrophage metalloelastase (MMP-12). MMP-12 represents an upregulated key enzyme in chronic obstructive pulmonary disease (COPD),[33,34,35] neurological diseases,[36] cancer[37,38] and in atherosclerosis.[39,40,41,42] PET imaging of atherosclerosis is a particular focus of our group. In general the imaging of single MMPs is challenging because in comparison to an imaging approach of the whole MMP enzyme family the absolute amount of activated enzyme (and for this reason B_{max}) is decreased. Under the assumption that a B_{max}/K_i ratio ≥ 10 is sufficient for MMP imaging with nuclear medicine techniques a potent MMPI radiotracer (with a low K_i-value) that is specific for the relevant MMP must be available.[43,44,45] Under these premises the imaging of a single MMP gives the great opportunity to evaluate the role of this specific MMP in specific biological processes (e.g. pathological situations) resulting in possibilities to manipulate this processes with targeted interactions with the specific MMP (e.g. potential therapy approaches associated with single MMPs). For MMP-12 the situation is additionally complicated because the enzyme can be located intra- and extracellular and the availability of the enzyme for potential radiotracer binding is not equal in both environments.[46,47] Nevertheless latest papers showed that SPECT/PET-imaging of specific MMPs (families) is feasible even in a COPD mice model that is closely associated with the overexpression of activated MMP-12.[48,49]

For our purposes, the dibenzofuransulfonamide-based MMPIs, selectively inhibiting MMP-12 and discovered by Wu *et al.* (e.g. **MMP118** in Figure 2)[50], were chosen as lead compounds for further (radio)chemical modifications.

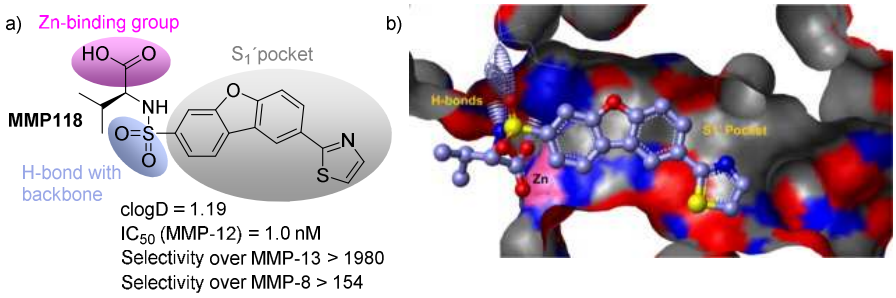

Figure 2. a) Lead compound **MMP118**, b) X-ray co-crystal structure of **MMP118** and MMP-12 adapted from Wu *et al.*[50]

In contrast to the above mentioned agents CGS 27023A and CGS 25966 the dibenzofuransulfonamide-based MMPIs possess a carboxylic acid moiety as Zn-binding group while the O-atoms of the sulfonamide group interact with the amino acid backbone of the enzyme *via* hydrogen bonding. The dibenzofuran scaffold or core substituted with a five-membered heterocycle occupies the S1´-pocket of MMP-12. The thiazolyl-substituted lead compound **MMP118** demonstrates more than 150-fold selectivity over the structurally related MMP-8 and -13.

RESULTS AND DISCUSSION

Chemistry. In the first step of the development of potent and selective MMP-12 radiotracers for PET imaging labeled with fluorine-18 and based on the described dibenzofuransulfonamide lead structure the corresponding non-radioactive counterparts substituted with fluorinated five-membered heterocycles were synthesized and tested in *in vitro* MMP assays.

Thus, the aryl bromide key intermediate **1** was synthezised in 5 steps with an overall yield of 52% from dibenzofuran according to a procedure reported in literature.[50,51] Aryl bromide **1** was converted into the corresponding azide **2** with sodium azide and CuI as catalyst. After copper(I)-

catalyzed Huisgen azide-alkyne 1,3-dipolar cycloaddition ("click-reaction") with 5-fluoropent-1-yne[22] yielding triazole **3**, the *tert*-butyl ester was cleaved with KSF clay in acetonitrile under reflux. The resulting target compound **4** was obtained with 37% yield over 3 steps. Moreover precursor **5** for potential labeling with 5-[^{18}F]fluoropent-1-yne was also prepared by ester cleavage of **2** with KSF clay in acetonitrile (Scheme 1).

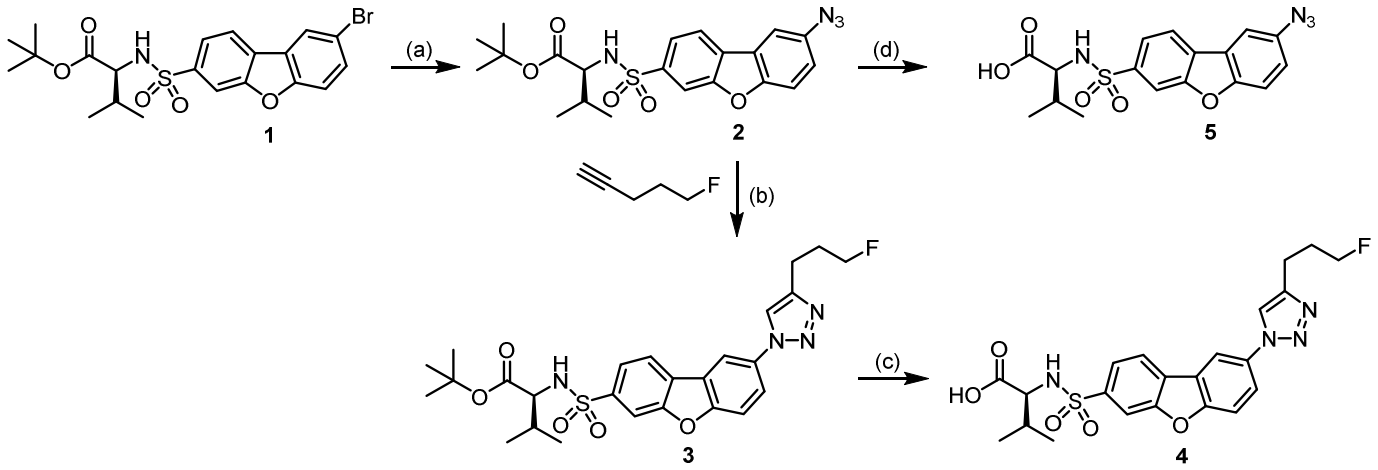

Scheme 1. Synthesis of *N*-linked triazole derivative **4**. Reagents and conditions: (a) NaN_3, Na ascorbate, CuI, DMEDA, EtOH/H_2O (7:3), 100 °C, 30 min, 94%; (b) Na ascorbate, CuI, DMF, rt, 4 h, 49%; (c) KSF clay, CH_3CN, 100 °C, 6 h, 81%; (d) KSF clay, CH_3CN, 100 °C, 5 h, 79%.

The synthesis of the *C*-linked triazole derivative **9** also started with the aryl bromide **1** (Scheme 2). After Sonogashira coupling of **1** with trimethylsilylacetylene, the silyl group was cleaved from **6** under basic conditions similar to a procedure described in the literature[52] to yield alkyne **7**. Subsequent 1,3-dipolar cycloaddition of alkyne **7** with 2-fluoroethyl azide provided the *C*-linked triazole **8**. Finally the *tert*-butyl ester **8** was hydrolyzed with KSF clay and the *C*-linked triazole **9** was obtained in 42% over the the described four reaction steps. Furthermore the

potential precursor **10** for radiolabeling with 2-[^{18}F]fluoroethyl azide[22,53] was prepared analogously from **7** by cleavage of the ester group with KSF clay and 71% yield.

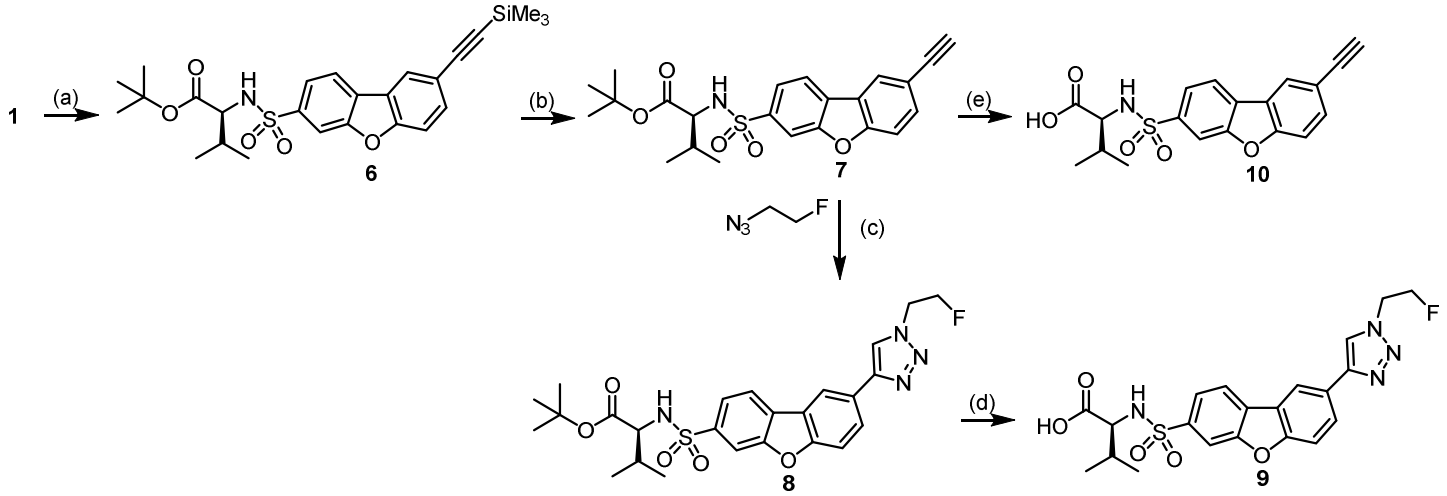

Scheme 2. Synthesis of *C*-linked triazole derivative **9**. (a) $(Me)_3SiC{\equiv}CH$, $PdCl_2(PPh_3)_2$, CuI, Et_3N, DMF, 65 °C, 16 h, 68%; (b) K_2CO_3, MeOH, rt, overnight, 94%; (c) Na ascorbate, CuI, DMF, rt, 4 h, 83%; (d) KSF clay, CH_3CN, 100 °C, 6 h, 80%; (e) KSF clay, CH_3CN, 100 °C, 5 h, 71%.

To elucidate the influence of different Zn-binding groups, the carboxylic acids **4** and **9** were converted into the corresponding hydroxamates **12a-b** by coupling with *O*-THP hydroxylamine and subsequent cleavage of the THP protective group with HCl in dioxane (Scheme 3). The overall yield of the *N*-and *C*-linked triazoles **12a** and **12b** containing the hydoxamate Zn-binding moiety was 51% and 65%, respectively.

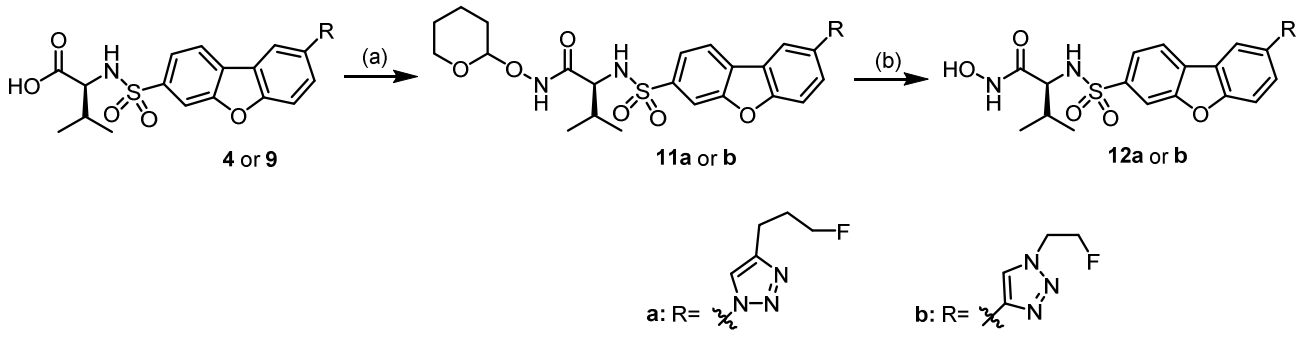

Scheme 3. Conversion of the carboxylic acids **4** and **9** into hydroxamic acids **12a** and **12b**. (a) $THPONH_2$, HOBT, NMM, EDC, DMF, rt, overnight, **11a** 96%, **11b** 87%; (b) 4 M HCl in dioxane, rt, 2 h, **12a** 53%, **12b** 75%.

For the preparation of dibenzofuransulfonamides substituted with fluorinated pyrazoles the brominated pyrazol derivates **13** and **14** were prepared from 2-fluoroethyl tosylate and the corresponding 3-bromo- and 4-bromopyrazole *via* nucleophilic substitution under basic reaction conditions (Scheme 4).

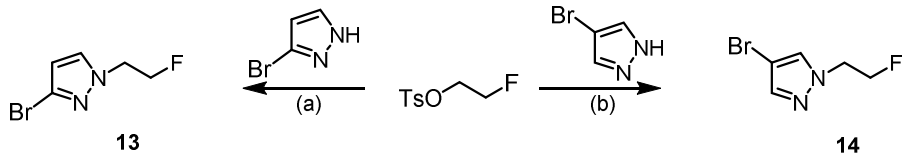

Scheme 4. Synthesis of brominated (2-fluoroethyl)pyrazoles **13** and **14**. (a) Cs_2CO_3, DMF, 100 °C, 3 h, 51%; (b) Cs_2CO_3, DMF, 100 °C, 6 h, 56%.

The (*S*)-enantiomer of the arylboronic acid pinacol ester **15** prepared according to a literature protocol[51] was reacted with bromopyrazoles **13** and **14** in a Suzuki-Miyaura reaction to afford the coupling products **16** and **18**. Cleavage of the *tert*-butyl ester of **16** and **18** with KSF clay in acetonitrile led to the carboxylic acids **17** and **19** with overall yields of 37 and 38%, respectively

(Scheme 5). In order to study the significance of the configuration of the center of chirality in this class of MMP inhibitors *ent*-**19**, the (*R*)-configured enantiomer of **19**, was prepared in the same manner starting from the pinacol ester *ent*-**15** in two steps with an overall yield of 7%.

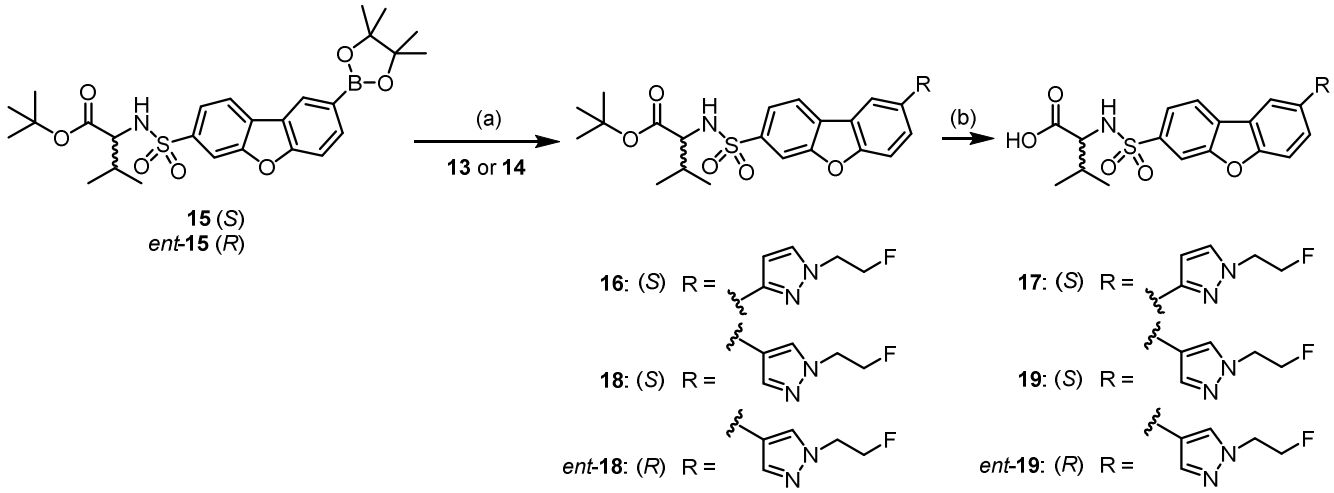

Scheme 5. Synthesis of fluorinated pyrazole substituted derivatives **17**, **19** and *ent*-**19**. (a) K_2CO_3, $PdCl_2(PPh_3)_2$, DME/H_2O (7:1), 85 °C, 3-5 h, **16** 51%, **18** 47%, *ent*-**18** 21%; (c) KSF clay, CH_3CN, 100 °C, 5 h, **17** 72%, **19** 80%, *ent*-**19** 34%.

Moreover, arylboronate **15** was used for the preparation of the tosylate precursor **22** for the synthesis of the fluorine-18 labeled MMP-12 inhibitor **[^{18}F]19**. For this purpose, 4-bromopyrazole was alkylated with ethylene sulfate followed by tosylation of the hydroxy group of alcohol **20**. The final Suzuki-Miyaura coupling of the arylboronic acid pinacol ester **15** with tosylate **21** provided the desired precursor **22** with 9% yield over three steps (Scheme 6).

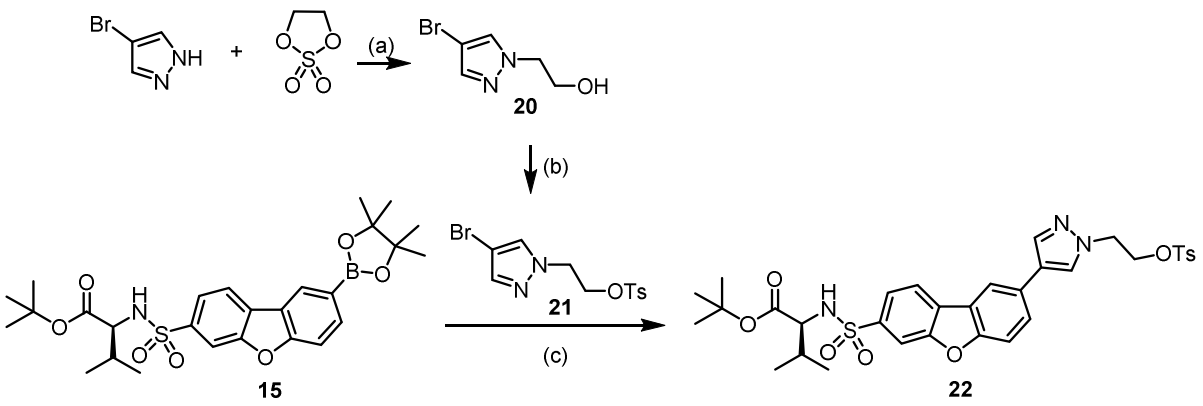

Scheme 6. Preparation of the precursor **22** for radiosynthesis of **[^{18}F]19**. (a) KO^{t}Bu, DMF, rt, overnight, 57%; (b) TsCl, NEt_3, CH_2Cl_2, rt, 20 h, 50%; (c) K_2CO_3, $PdCl_2(PPh_3)_2$, DME/H_2O (7:1), 85 °C, 5 h, 30%.

Analog to Scheme 6 the preparation of the corresponding tosylate substituted ester that can serve as potential precursor for fluorine-18 labeled **[^{18}F]17** could not be realized because a product mixture was obtained that could not be sufficiently purified.

Additionally three fluorinated thiazoles **25**, **28** and **31** and a thiophene derivative **34** were synthesized starting with the Suzuki-Miyaura coupling of pinacol ester **15** with the corresponding brominated hydroxyethyl thiazole or thiophene derivatives and microwave heating followed by nucleophilic substitution with DAST to yield fluorinated intermediats **24**, **27**, **30** and **33**. Finally, after cleavage of the *tert*-butyl ester with KSF clay the carboxylic acids **25**, **28**, **31** and **34** were obtained in overall yields of 17-37% (Scheme 7).

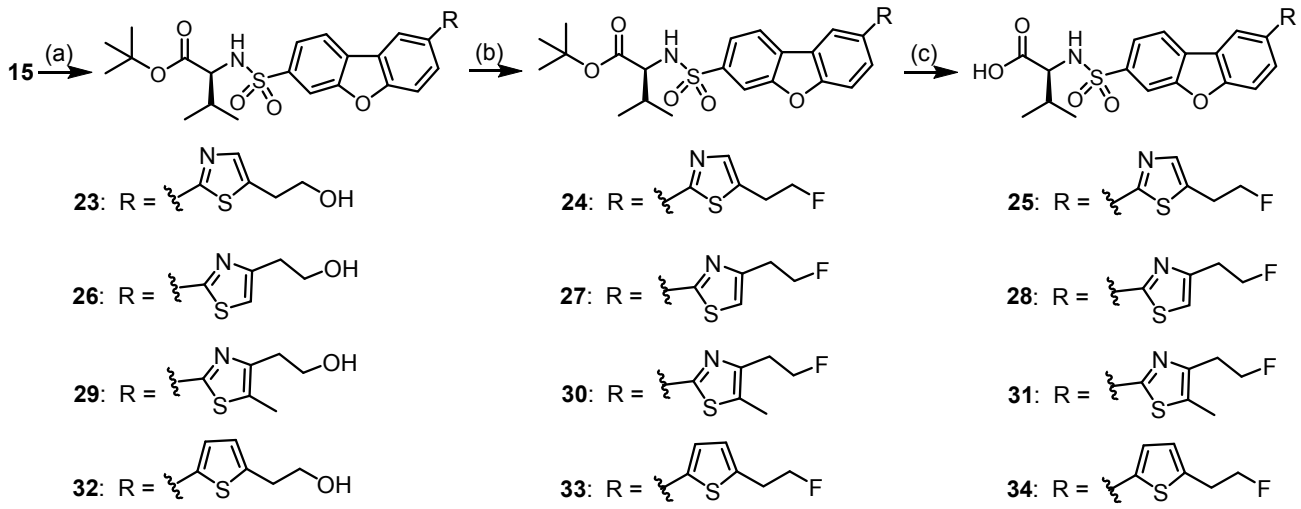

Scheme 7. Synthesis of fluorinated thiazolyl and thienyl substituted derivatives **25**, **28**, **31** and **34**. (a) brominated hydroxyethyl thiazole or thiophene derivative, K_2CO_3, $PdCl_2(PPh_3)_2$, DME/H_2O (7:1), microwave, 150 W, 100 °C, 20-180 min, **23** 49%, **26** 47%, **29** 66%, **32** 40%; (b) DAST, toluene, rt, overnight, **24** 82%, **27** 64%, **30** 80%, **33** 83%; (c) KSF clay, CH_3CN, 100 °C, 5 h, **25** 92%, **28** 56%, **31** 58%, **34** 54%.

***In vitro* MMP inhibition.** The MMP inhibition of synthesized fluorinated five-membered heteroaryl substituted dibenzofuransulfonamides **4**, **9**, **12a-b**, **17**, **19**, *ent*-**19**, **25**, **28**, **31** and **34** and the non heteroaryl substituted azide and alkyne derivatives **5** and **10** was recorded. The inhibition of activated MMP-2, -8, -9, -12 and -13 was investigated in a fluorometric *in vitro* inhibition assay according to a literature procedure.[54] Furthermore selected candidates (**4**, **9**) were tested in MMP-1, -3 and -7 assays. The obtained IC_{50}-values are listed in Table 1. In order to analyze changes in the lipophilicity/hydrophilicity caused by structural modifications the log$D_{7.4}$-values of the non-radioactive test compounds were determined by a micro-shake-flask method coupled with LC-MS quantification.[55] The log$D_{7.4}$ values of the radiolabeled analogs were determined by the shake-flask method with γ-counting based analysis.

Table 1. MMP inhibitory activity of fluorinated five-membered hetaryl substituted dibenzofuran sulfonamides **4**, **9**, **12a-b**, **17**, **19**, *ent*-**19**, **25**, **28**, **31** and **34** and the non heterocycle substituted azide and alkyne derivative **5** and **10**.

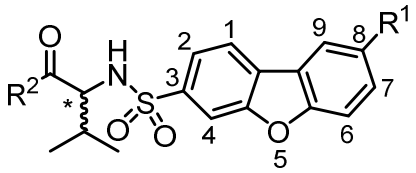

Cpd.	R^1	R^2	Config.	IC_{50} ± SD [nM]					$\log D_{7.4}$
				MMP-2	MMP-8	MMP-9	MMP-12	MMP-13	
4[c]	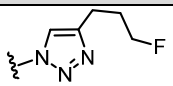	OH	(*S*)	81 ± 3	19 ± 3	2230 ± 1200	0.19 ± 0.02	288 ± 10	0.59± 0.07[a] 0.48± 0.01[b]
12a	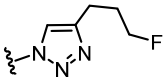	NHOH	(*S*)	2670 ± 449	421 ± 123	8760 ± 2390	62 ± 30	1170 ±341	2.55± 0.03[a]
9[d]	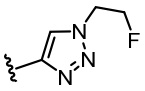	OH	(*S*)	35 ± 6	2.0 ± 0.6	>10000	$0.001 \pm 3 \cdot 10^{-5}$	16 ± 5	0.09± 0.07[a] 0.00± 0.01[b]
12b	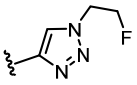	NHOH	(*S*)	174 ± 21	27 ± 11	>10000	3 ± 2	62 ± 15	2.33± 0.08[a]
17	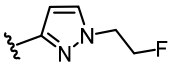	OH	(*S*)	6.5 ± 3	8.5 ± 0.7	413 ± 317	$0.0008 \pm 2 \cdot 10^{-4}$	2.4 ± 0.4	0.73± 0.02[a]
19	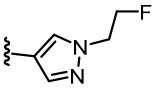	OH	(*S*)	0.84 ± 0.03	0.18 ± 0.02	151 ± 5	$0.0004 \pm 1 \cdot 10^{-4}$	3.2 ± 0.08	0.68± 0.02[a] 0.63± 0.02[b]
ent-**19**	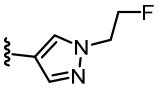	OH	(*R*)	2.0 ± 0.4	3.0 ± 0.3	n.d.	2.0 ± 0.1	19 ± 5	0.68± 0.02[a]
25	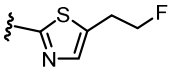	OH	(*S*)	26 ± 3	0.22 ± 0.03	n.d.	0.12 ± 0.04	332 ± 11	1.26± 0.01[a]
28	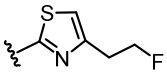	OH	(*S*)	55 ± 10	2.0 ± 0.6	195±33	0.081 ± 0.002	60 ± 4	1.25± 0.02[a]

31	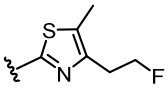	OH	(*S*)	0.49 ± 0.01	0.51 ± 0.3	200 ± 49	0.94 ± 0.13	12.0 ± 0.5	1.71± 0.02[a]
34	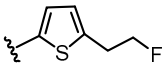	OH	(*S*)	20 ± 12	2.0 ± 0.4	58 ± 4	$0.001 \pm 2 \cdot 10^{-4}$	20 ± 3	1.70± 0.02[a]
5	N_3	OH	(*S*)	3 ± 0.5	2 ± 0.1	250 ± 2	1.0 ± 0.07	90 ± 4	-
10	C≡CH	OH	(*S*)	14 ± 0.3	22 ± 6	>1000	21 ± 6	406 ± 24	-

n.d. not possible to determine due to inhomogenous data

[a] $\log D_{7.4}$-values were determined by MS quantification (n = 9)

[b] $\log D_{7.4}$-values were determined using the radiolabeled analogs (n = 6)

[c] IC_{50}(MMP-1) > 10 µM, IC_{50}(MMP-3) = 4.2 ± 0.7 µM, IC_{50}(MMP-7) > 10 µM

[d] IC_{50}(MMP-1) > 10 µM, IC_{50}(MMP-3) = 4.2 ± 2.8 µM, IC_{50}(MMP-7) > 10 µM

In general, a suitable tool to modify MMP selectivity is the variation of the inhibitor P1´-substituent that occupies the S1´-cavity of MMPs. The S1´-pocket can be differentiated into small- (MMP-1, -7, -11, -20), medium- (MMP-2, -8, -9, -12, -14, -16) and large-sized (MMP-3, -10, -13)[56] and previous work of Li *et al.*[57,58] showed for the dibenzofuran based MMPIs that a C3/C8 substitution pattern is favored over a C2/C7 and a C3/C7 constellation regarding MMP-12 affinity and selectivity.

As shown in Table 1 all fluorinated heteroaryl substituted dibenzofurans with (*S*)-configuration and carboxylate moiety are excellent MMP-12 inhibitors with IC_{50}-values in subnanomolar to subpicomolar range (0.0004-0.94 nM for **4**, **9**, **17**, **19**, **25**, **28**, **31** and **34**). To the best of our knowledge, these compounds represent the most potent MMP-12 inhibitors reported so far in literature. The mentioned dibenzofurans also show MMP-2, -8 and MMP-13 inhibitory potency

in the nanomolar range (IC_{50}-values: 0.49-332 nM), but most of them (**4**, **9**, **17**, **19**, **34**) possess >100-fold selectivity for MMP-12 compared to the structurally related MMP-8 and -13 and the gelatinases MMP-2 and -9. Replacing the carboxylate Zn-binding group by a hydroxamate moiety led to a dramatic loss of MMP-12 inhibition (IC_{50}(**4**) = 0.19 nM; IC_{50}(**12a**) = 62 nM; IC_{50}(**9**) = 0.001 nM; IC_{50}(**12b**) = 3 nM). This is a remarkable fact because a contrary effect was observed for a selective peptide-based MMP-12 inhibitor.[59] Maybe this opposite effect for these different MMP-12 inhibitor classes (peptide-based and dibenzofuran-based) is caused by varied sterical interactions of the different S1´substituents in both inhibitor classes that must be shifted when the carboxylate moiety is displaced by a hydroxamate group. An additional effect is observed by inversion of the configuration. While (*S*)-configurated pyrazole **19** is a highly potent MMP-12 inhibitor (IC_{50} = 0.0004 nM), the (*R*)-configured enantiomer *ent*-**19** displays considerably decreased potency (IC_{50} = 2.0 nM). A similar observation was also reported by Wu *et al.*[50] for other derivatives of this compound class. Comparison of the compounds **28** and **31** reveals that the introduction of an additional methyl substituent at the terminal thiazole ring caused a 10-fold loss in MMP-12 inhibitory potency (IC_{50}(**28**) = 0.081 nM, IC_{50} (**31**) = 0.95 nM), but increased inhibitory activities against MMP-2, -8 and -13. The fundamental importance of the five-membered heterocycle for the MMP-12 selectivity was confirmed by azide **5** and alkyne **10**. Both compounds are potent inhibitors of MMP-2, -8 and -12 (IC_{50} = 1.0-22 nM) without designated inhibitory activities against MMP-9 and MMP-13. Compounds **4** and **9** were also tested against MMP-1, -3 and -7 with a designated small-sized (MMP-1, -7) and large-sized (MMP-3) S1´-pocket to demonstrate broad MMP-12 selectivity exemplarily. Consistent with previous results[50,57,58] both compounds showed little to no affinity for MMP-1 and -7 (IC_{50} > 10

μM) while a moderate inhibition of MMP-3 with a large-sized S1´-cavity was observed (IC_{50}(**4**) > 4.2 ± 0.7 μM, IC_{50}(**9**) > 4.2 ± 2.8 μM).

The hetaryl substituted dibenzofurans showed moderate lipophilicity with log$D_{7.4}$ values ranging from 0.09 to 2.55. Additionally, the log$D_{7.4}$ values of radiofluorinated analogues [^{18}**F**]**4**, [^{18}**F**]**9** and [^{18}**F**]**19** were determined (see section Radiochemistry). The log$D_{7.4}$ values recorded with the LC-MS for the non-radioactive analogs **4**, **9**, and **19** were in good accordance with the radiochemically determined values and differed by ≤0.11 units.

Based on these results the ^{18}F-labeled counterparts of *N*-linked triazole **4**, which was the first potent and selective MMP-12 inhibitor in our hands, *C*-linked triazole **9** and the most potent and extremely selective MMP-12 inhibitor **19** were chosen for radiosynthesis and further *in vitro*/*in vivo* evaluation. Radiosynthesis of **[^{18}F]17** whose non-radioactive analog **17** showed comparable MMP-12 affinty and selectivity to **19** was prevented due to the failed synthesis of a potential labeling precursor (see above).

Radiochemistry. The radiosyntheses of **[^{18}F]4**, **[^{18}F]9** and **[^{18}F]19** were carried out in a semiautomated two step procedure using a modified PET tracer radiosynthesizer TRACERLab FX_{FDG} (GE Healthcare).

The first step of the preparation of **[^{18}F]4** was the nucleophilic substitution at the precursor pent-4-yn-1-yl 4-methylbenzenesulfonate with anhydrous [^{18}F]fluoride yielding 5-[^{18}F]fluoropent-1-yne according to previous literature.[22] The second step consisting of the Cu(I)-catalyzed Huisgen azide-alkyne 1,3-dipolar cycloaddition of azide **5** and 5-[^{18}F]fluoropent-1-yne was conducted outside the automated system after distillation of 5-[^{18}F]fluoropent-1-yne in a separate flask with

cooled DMF (-10 °C) and addition of Cu(II)-sulfate pentahydrate and sodium ascorbate (Scheme 8).

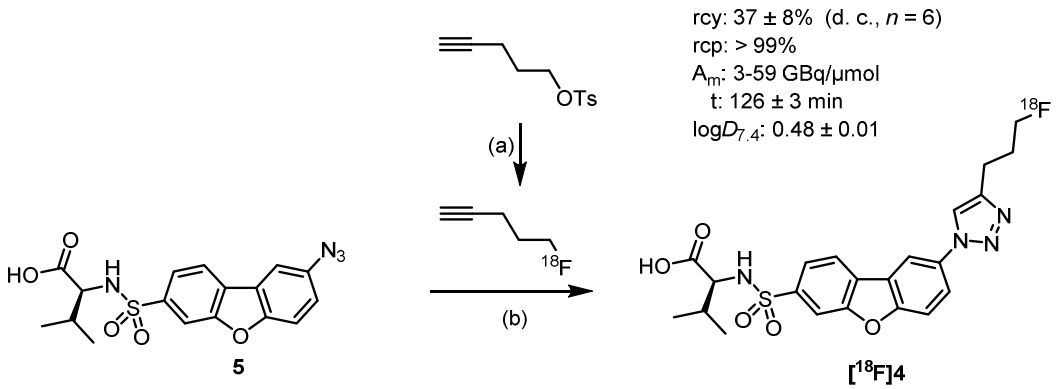

Scheme 8. Radiosynthesis of **[^{18}F]4**. (a) K(K_{222})[^{18}F]F, K_2CO_3, CH_3CN, 110 °C, 180 s; (b) $CuSO_4 \cdot 5H_2O$, Na ascorbate, DMF, 40 °C, 30 min.

After stirring for 30 min at 40 °C, purification by semipreparative HPLC, concentration and formulation, the product **[^{18}F]4** was obtained with overall radiochemical yield (rcy) of 37 ± 8% (decay corrected (d. c.), n = 6) in 126 ± 3 min with radiochemical purity (rcp) >99% and molar activity (A_m) of 3-59 GBq/µmol. The radiochemically determined log$D_{7.4}$-value of **[^{18}F]4** was 0.48 and differed just by 0.11 from the log$D_{7.4}$-value determined by MS quantification of compound **4**.

The radiosythesis of the *C*-linked triazole **[^{18}F]9** was performed in a similar way as the synthesis of the *N*-linked derivative **[^{18}F]4**. After preparation of 1-azido-2-[^{18}F]fluoroethane from 2-azidoethyl 4-methylbenzenesulfonate following the procedure of Glaser and Årstad with the improvement of Hugenberg *et al.*[22,53] Cu(I)-catalyzed 1,3-dipolar cycloaddition of precursor **10** with 1-azido-2-[^{18}F]fluoroethane yielded the desired radiofluorinated triazole **[^{18}F]9**. (Scheme 9)

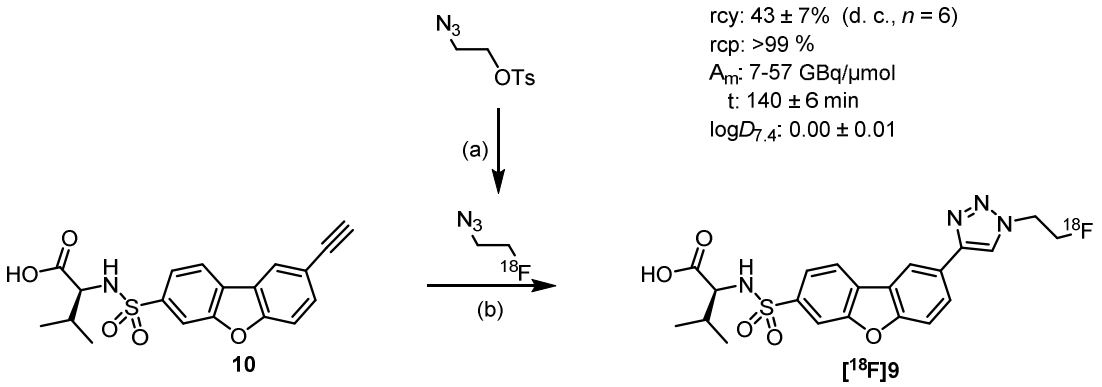

Scheme 9. Radiosynthesis of **[^{18}F]9**. (a) K(K_{222})[^{18}F]F, K_2CO_3, CH_3CN, 110 °C, 180 s; (b) $CuSO_4 \cdot 5H_2O$, Na ascorbate, DMF, 40 °C, 30 min.

After purification and formulation, the radiotracer **[^{18}F]9** was obtained in overall radiochemical yield of 43 ± 7% (decay corrected, n = 6) in 140 ± 6 min with radiochemical purity >99% and molar activity of 7-57 GBq/µmol. The log$D_{7.4}$-value of **[^{18}F]9** was 0.00 and differed only slightly from the log$D_{7.4}$-value determined for the non-radioactive analog **9** (0.09).[55]

The radiolabeling of the pyrazole derivative **[^{18}F]19** was also performed in two steps *via* nucleophilic substitution of the tosyloxy moiety of precursor **22** with anhydrous [^{18}F]fluoride and subsequent hydrolysis of the *tert*- butyl ester with TFA (Scheme 10).

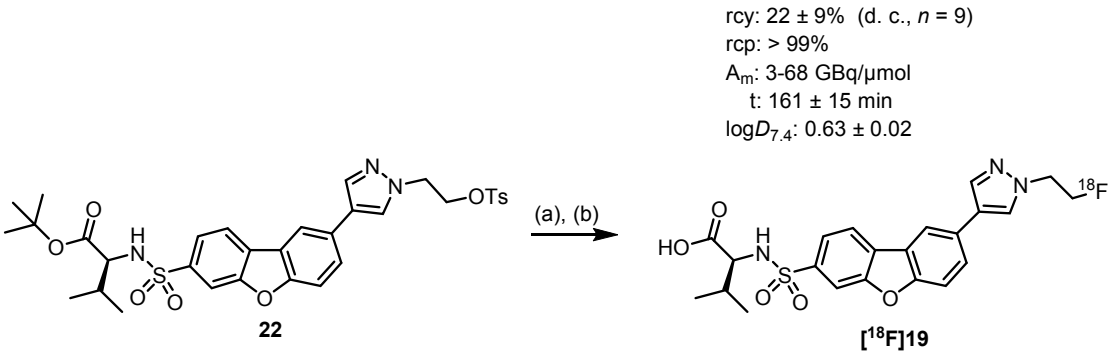

Scheme 10. Radiosynthesis of **[^{18}F]19.** (a) K(K_{222})[^{18}F]F, K_2CO_3, CH_3CN, 100 °C, 30 min; (b) TFA, 40 °C, 5 min.

After purification and formulation, the pyrazole derivative **[^{18}F]19** was received in overall radiochemical yield of 22 ± 9% (decay corrected, n = 9) in 161 ± 15 min with radiochemical purity >99% and molar activity of 3-68 GBq/µmol. The log$D_{7.4}$-values of **19** and **[^{18}F]19** determined by different methods were almost identical (0.68 *vs.* 0.63).

***In vitro* stability in human and mouse serum**. The *in vitro* stability was investigated by incubation of the three radiotracers with human and mouse blood serum. All three tracers **[^{18}F]4, [^{18}F]9** and **[^{18}F]19** revealed excellent serum stability upon incubation up to 90 min at 37 °C. Only the parent compounds without any radiometabolites or decomposition products were detected by analytical radio-HPLC. Figure 3 shows exemplarily the radio-HPLC chromatograms of **[^{18}F]4**, **[^{18}F]9** and **[^{18}F]19** after incubation with mouse serum for 90 min.

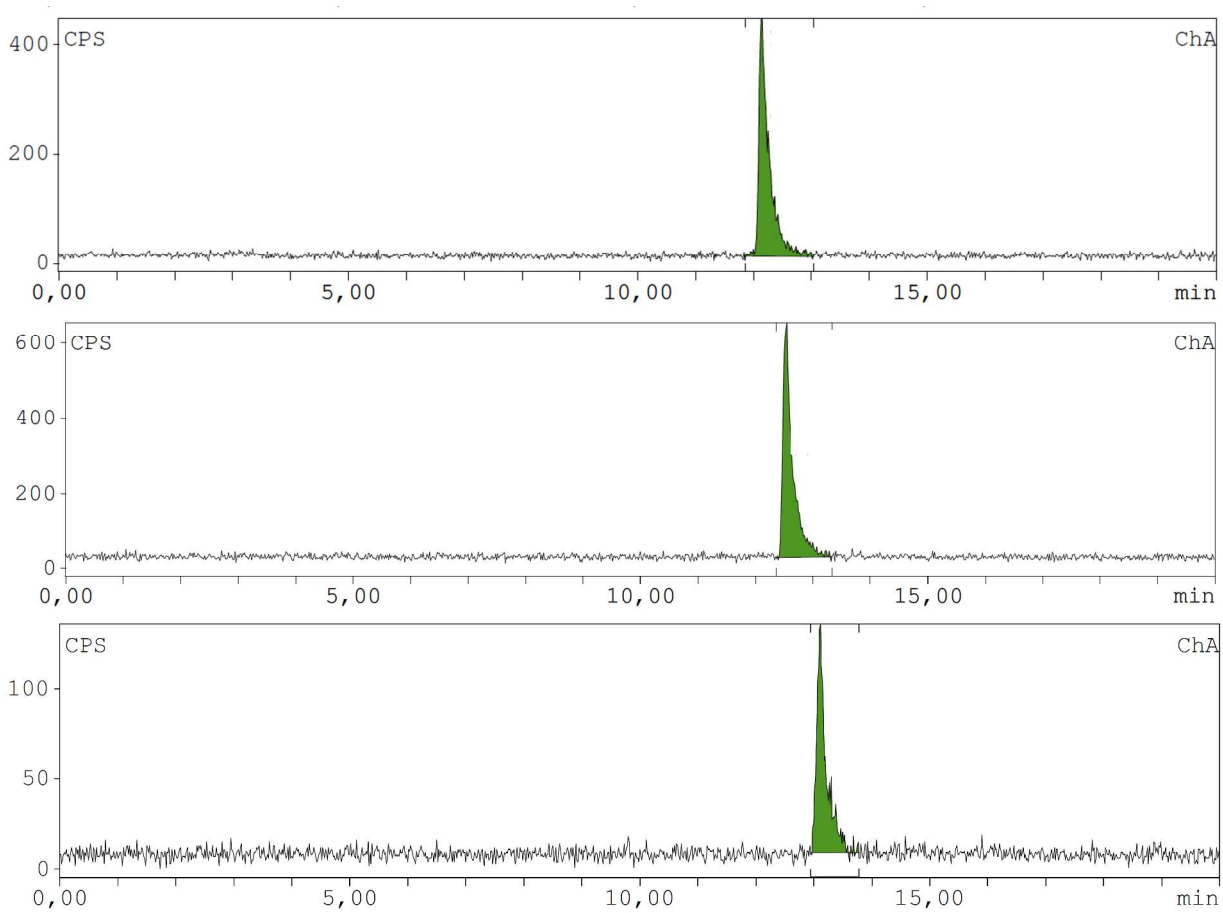

Figure 3. Serum stability: radio-HPLC chromatograms after incubation of **[^{18}F]4** (top), **[^{18}F]9** (middle) and **[^{18}F]19** (bottom) with mouse blood serum at 37°C for 90 min. Radio-HPLC: Method D.

***In vitro* biotransformation using mouse liver microsomes.** To identify metabolically labile structural elements as early as possible, the carboxylic acids **4**, **9** and **19** as well as the hydroxamic acids **12a** and **12b** were incubated with mouse liver microsomes and NADPH/H^+ with and without UDPGA (UDP-activated glucuronic acid) for 2 h. The formation of metabolites was monitored by LC coupled with quadrupole-time-of-flight-MS (qToF) allowing identification of metabolite structures by analysis of the exact masses of separated compounds and generated fragments ions.

Incubation of hydroxamates **12a** and **12b** with mouse liver microsomes and NADPH/H^+ led to formation of the carboxylic acids **4** and **9** (phase 1 metabolites), respectively. In addition to the acids **4** and **9**, conjugation products **35a** and **35b** (phase 2 metabolites) were detected after incubation of **12a** and **12b** with UDPGA and NADPH/H^+. Both types of metabolites originate from transformation of the hydroxamic acid. (Scheme 11)

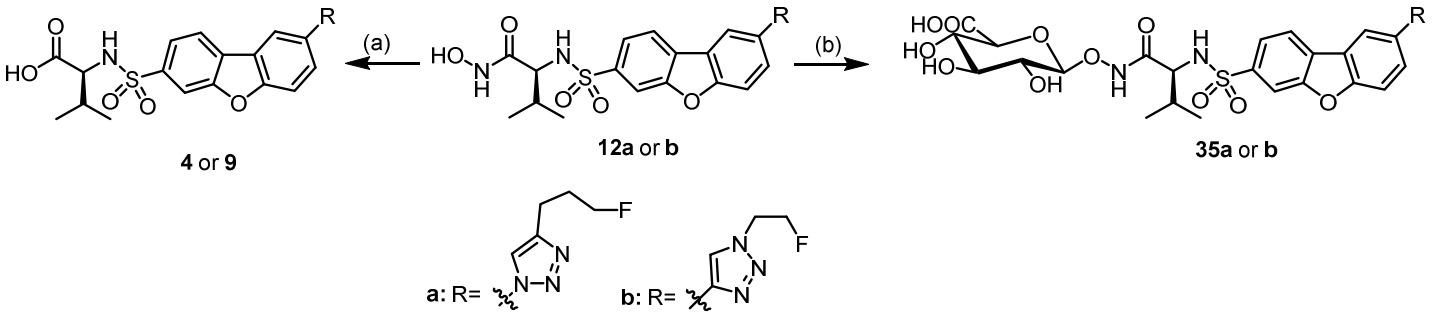

Scheme 11. Metabolites of hydroxamates **12a-b** in the mouse liver microsome assay. (a) mouse liver microsomes, NADPH/H^+, rt, 2 h; (b) mouse liver microsomes, NADPH/H^+, UDPGA, rt, 2 h.

Incubation of the acids **4**, **9** and **19** with mouse liver microsomes and different cofactors did not lead to metabolites in reasonable amounts. The missing metabolites indicate a very high metabolic stability that can be explained by the absence of the hydroxamate functional group, and thus represents a promising starting point for *in vivo* experiments.

Due to the extraordinarily high potency of the pyrazole **19** (MMP-12: IC_{50} = 0.4 pM) a sample was incubated with cofactors NADPH/H^+ and UDPGA for 90 min and subsequently analyzed using higher injection volumes in order to detect metabolites formed only in trace amounts. The extracted ion chromatogram (EIC, Figure 4) shows in addition to the peak of the parent compound **19** two small peaks indicating two metabolites in trace amounts. Although peak sizes

can be compared only supposing a similar ability to be ionized in ESI positive mode, the very small peaks of the metabolites reveal high metabolic stability of **19** (Figure 4).

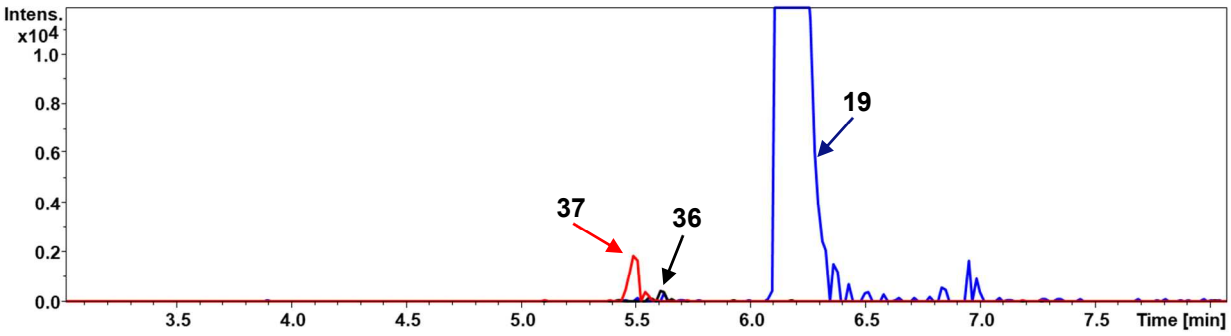

Figure 4. Extracted ion chromatograms (EICs, ESI positive mode) of parent compound **19** (*m/z* 460.1319 ± 0.01) and metabolites **36** (*m/z* 476.1246 ± 0.01) and **37** (*m/z* 636.1673 ± 0.01), 90 min after incubation with mouse liver microsomes, NADPH/H^+ and UDPGA. HPLC-MS: Method F.

The structures of the formed metabolites **36** and **37** were identified by fragmentation experiments (MRM) (Figure 5). Whereas the first metabolite **36** was generated by oxidation of the isopropyl moiety (phase 1 metabolite), conjugation with glucuronic acid led to the glucuronide **37** (phase 2 metabolite). The high metabolic activity of the used murine microsomes and incubation conditions have already been described.[60,61]

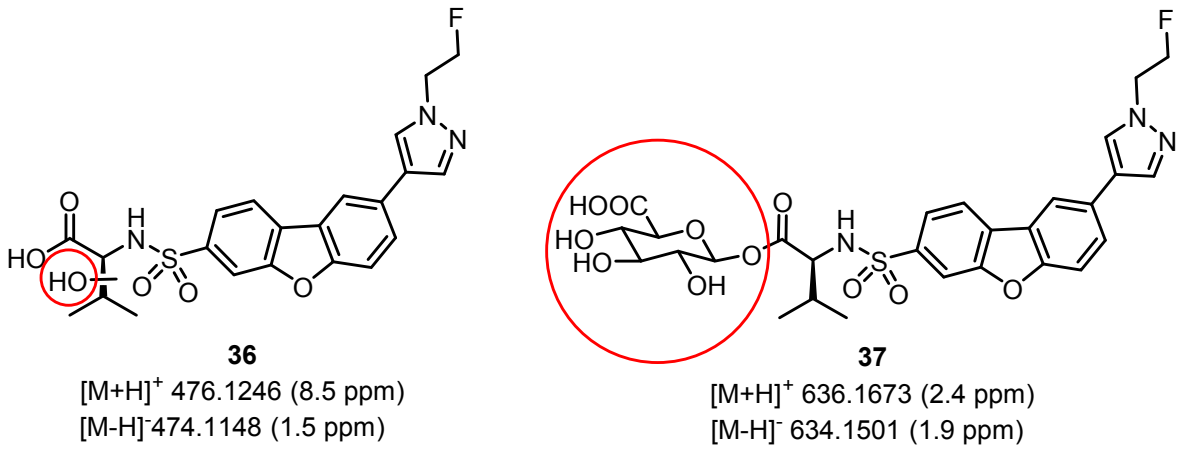

Figure 5. Postulated metabolites formed upon incubation of **19** with mouse liver microsomes, NADPH/H^+ and UDPGA.

***In vitro* binding to human serum albumin.** *In vitro* human serum albumin (HSA) binding of triazoles **4** and **9** as well as pyrazoles **17** and **19** was investigated by high performance affinity chromatography (HPAC) using an analytical HPLC column coated with HSA. HSA was selected as it is, together with α1-acid glycoprotein (AGP), mainly responsible for plasma protein binding (PPB) and represents the main plasma protein.[62,63] The retention factor k´ of a compound correlates with its HSA binding, since it reflects the interactions with the stationary phase. At first, the retention factors of compounds with known HSA binding were determined to generate a calibration curve that allowed the calculation of HSA binding (in %) of unknown compounds after measurement of their k´-values.[64] According to this procedure more than 90% HSA binding was recorded for all four compounds (**4**: 98%; **9**: 94%; **17**: 97%; **19**: >99%) indicating high HSA binding and thus high PPB of the investigated MMP-12 inhibitors.

***In vivo* Biodistribution Studies.** The *in vivo* biodistribution studies of all three fluorine-18 labelled compounds **[^{18}F]4**, **[^{18}F]9** and **[^{18}F]19** were investigated in adult C57BL/6 mice (n = 2)

after intravenous injection of 3-11 MBq as 120 min dynamic PET scans. Representative horizontal and sagittal slices and maximum intensity projections (MIP) of whole body images at selected time points after tracer injection are represented in Figure 6.

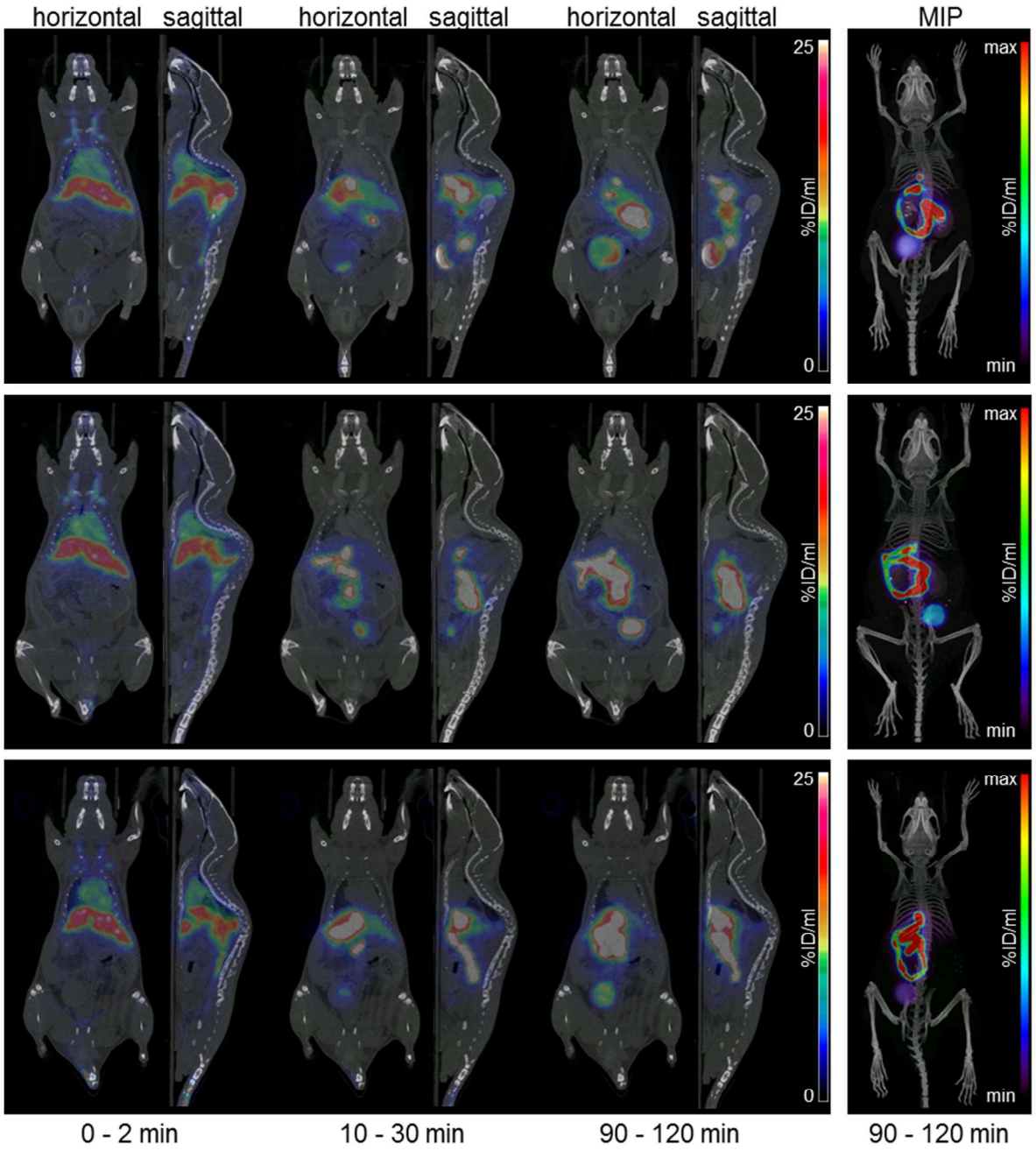

Figure 6. Horizontal/sagittal slices and maximum intensity projection of the *in vivo* biodistribution of tracer-associated radioactivity in an adult C57BL/6 mouse after intravenous injection of **[^{18}F]4** (8.3 MBq, top), **[^{18}F]9** (10.8 MBq, middle) and **[^{18}F]19** (9.2 MBq, bottom).

The biodistributions of the three radiotracers are very similar to each other, no significant differences were observed. All tracers showed very fast and efficient elimination from the body. Shortly after injection, a high accumulation of radioactivity was observed in the liver followed by accumulation in the interstine. On the other side a comparatively low accumulation in the kidneys and the bladder was found pointing to a predominate hepatobiliary excretion. Accumulation of radioactivity in the bones, indicating free [^{18}F]fluoride ions, was not observed in the entire dynamic imaging study. Additionally the PET image data were analyzed quantitatively for selected regions of interest (Figure 7).

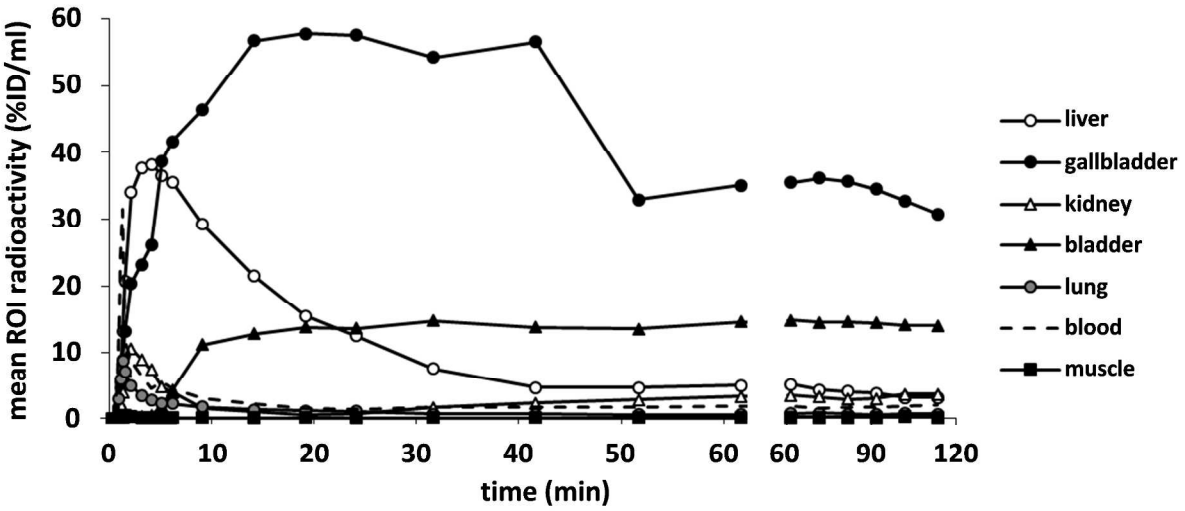

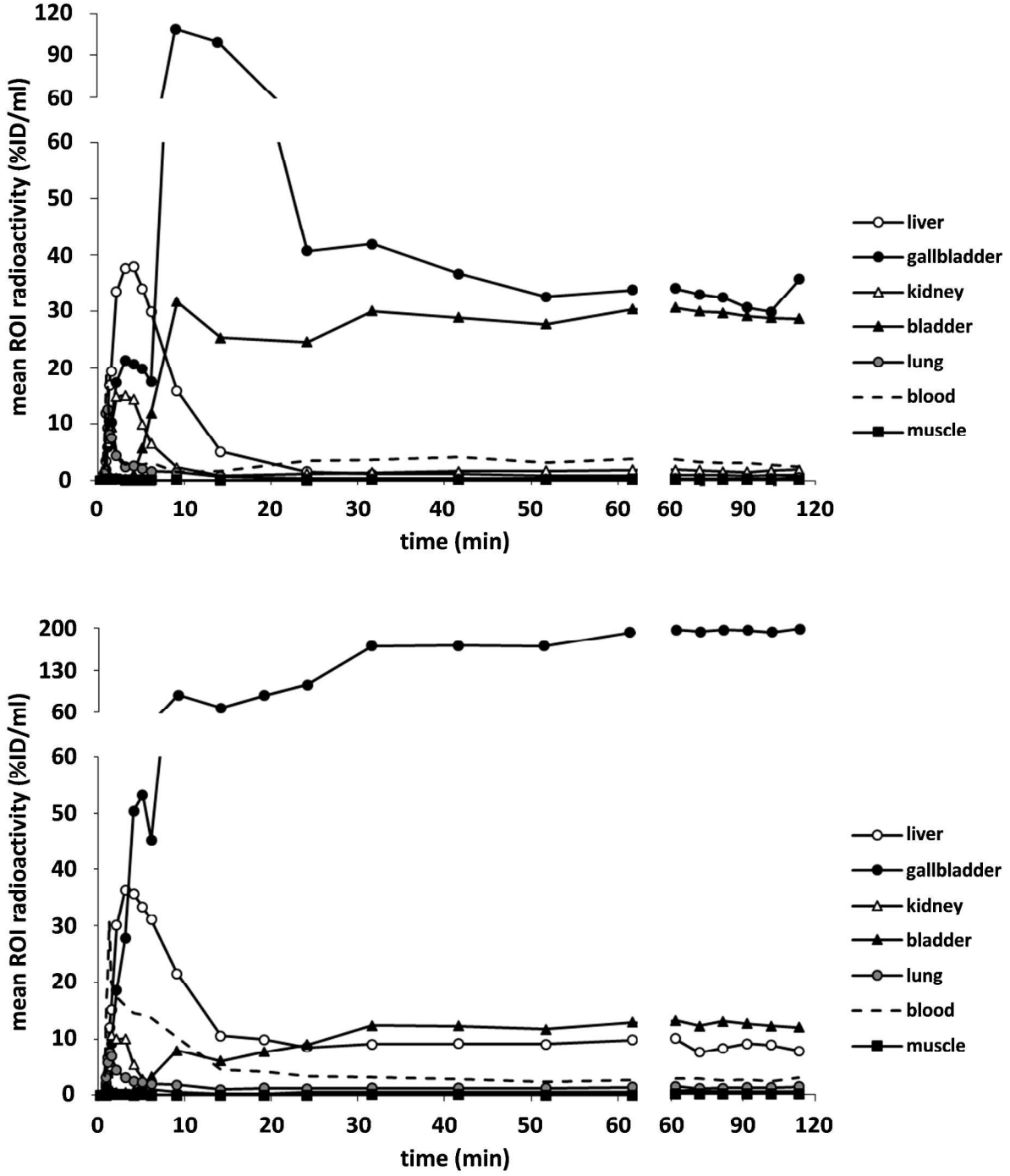

Figure 7. *In vivo* biodistribution of radioactivity in an adult C57BL/6 mouse after intravenous injection of **[^{18}F]4** (top), **[^{18}F]9** (middle) and **[^{18}F]19** (bottom). Time-activity curves illustrate tracer dynamics in selected regions of interest (ROI). Activity is displayed as percentage of injected dose per volume during the whole observation period of 120 min.

According to predominant hepatobiliary excretion of the three compounds the highest activity concentrations were found in the liver (35-40%ID/mL) and gallbladder (>40%ID/mL) within the first 10 minutes after injection. Subsequent decrease of liver activity to less than 10% ID/mL reflects the continuous clearance of all three compounds until the end of the study. Gallbladder activity varied between the biodistribution studies, typically due to inter-individual different secretory stimuli under anesthesia. The activity of **[^{18}F]19** in the gallbladder persists throughout the imaging study of 120 minutes. One might speculate that this pattern could be explained by the inter-individual variation or different hydration states at the day of PET imaging. However a tracer specific characteristic as a cause for the persistance in the gallbladder can not be excluded After initial activity peaks in blood (18-31%ID/mL) and lungs (<15%ID/mL) in the first five minutes, only a low amount of radioactivity (<3%ID/mL) was observed in non-excretion organs or tissues such as brain, lung, heart, spleen, and muscles (exemplarily data of muscles are shown). Similarily, the activity concentration in the kidneys decreased after an initial peak (10-15%ID/mL) to <5%ID/mL for the period 10-120 min while the bladder activity concentration remained between 10 and 30%ID/mL for the later time points (30-120 min). The high HSA binding determined in the section "*in vitro* binding to human serum albumin" for non-radioactive counterparts **4**, **9**, and **19** prevented not the efficient washout of labeled analogs **[^{18}F]4**, **[^{18}F]9** and **[^{18}F]19** from the blood shown by limited blood activities of <5%ID/mL already after 20 min.

CONCLUSION

This study aimed at the development of PET tracers for imaging of activated MMP-12 that is a promising target in different pathologies. Therefore, this work presented in the first step the successful syntheses of dibenzofuransulfonamidecarboxylic acid based MMP-12 inhibitors with

(*S*)-configuration and terminal triazole (**4**, **9**), pyrazole (**17**, **19**), thiazole (**28**, **31**) and thiophene (**37**) rings with fluoroalkyl substituent. The compounds revealed excellent inhibitory potential (IC_{50}-values: 0.0004-0.19 nM) and high selectivity (≥ 25 fold) for MMP-12. To the best of our knowledge these compounds represent the most potent MMP-12 inhibitors decribed in literature so far. Changing the Zn-binding group to a hydroxamic acid moiety (**12a-b**), inversion of the center of chirality to (*R*)-configuration (**22**), adding an additional substituent at the terminal five-membered heterocycle (**34**) or substitution of core sytem by an azide (**5**) or alkyne group (**10**) led to dramatic loss of MMP-12 inhibition and selectivity for MMP-12. Moreover, **4**, **9** and **19** showed high HSA-binding (≥94%) and high metabolic stability upon incubation with mouse liver microsomes. Due to this preliminary results compounds **4**, **9** and **19** were selected for radiochemical resyntheses. The fluorine-18 labeled and moderate lipophilic analogs **[^{18}F]4**, **[^{18}F]9** and **[^{18}F]19** (log$D_{7.4}$ 0.00-0.63) were successfully synthesized radiochemically in two step procedures with rcy of 22-43% (d. c.). The triazoles **[^{18}F]4** and **[^{18}F]9** and the pyrazole **[^{18}F]19** showed excellent stability *in vitro*, when incubated with human and mouse serum without formation of fragments and/or metabolites. Initial biodistribution studies of all three radiotracers in C57BL/6 mice using small animal PET exhibited predominantly hepatobiliary elimination of the radiofluorinated inhibitors without undesired and unspecific accumulation in non-excretion organs and bones indicating non-formation of [^{18}F]fluoride. In summary **[^{18}F]4**, **[^{18}F]9** and **[^{18}F]19** featured promising *in vitro* and *in vivo* behavior predetermining these MMP-12 inhibitors for further *in vivo* evaluation with PET in mouse models that are characterized by elevated levels of activated MMP-12 such as the models of irritant contact determititis (ICD) and collagen induced arthritis (CIA).

EXPERIMENTAL SECTION

Chemistry: General Methods

All purchased chemicals, reagents and solvents for synthesis were of analytical grade quality and applied without further purification. Demineralized water was used if not otherwise mentioned. For radiosynthesis water of injection was used and DNA-grade CH_3CN. Air and moisture-sensitive reactions were handled under argon atmosphere. The microwave reactions were performed with Discover SP – Microwave Synthesizer (CEM). Parameters such as solvent, power, temperature, and time are declared in the synthetic procedures. Melting points (mp) are uncorrected and were measured with melting point system Stuart SMP 3 (STUART SCIENTIFIC) and melting point system mp 70 (METTLER TOLEDO) using an open capillary. GC/MS measurements were performed with GC system GC-2010 couplet with mass spectrometer GCMS-QP2010 (SHIMADZU). Column Rxi-1ms (30.0 m length, 0.25 mm internal diameter, 0.25 µm thickness, RESTEK) was used and helium as carrier gas. Data acquisition were realized with GCMS solution version 2.71 software (SHIMADZU). Thin layer chromatography was performed with TLC silica gel sheets POLYGRAM® SIL G/UV_{254} (MACHEREY-NAGEL). As stationary phase for the flash column chromatography silica gel 60 (40 – 63 µm, Merck) was used. Pressure was applied with compressed air. Eluent and the retention factor (R_f) are declared in the synthetic procedures. Automatic flash column chromatography was performed with Reveleris X2 (GRACE, now BÜCHI). As stationary phase silica flash cartridges were used. Parameters such as cartridge, flow rate and eluent are declared in the synthetic procedures. NMR spectra were recorded on an AV300 (^{1}H NMR 300 MHz, ^{13}C NMR 75 MHz, ^{19}F NMR 282 MHz) or AV400 (^{1}H NMR 400 MHz, ^{13}C NMR 100 MHz) spectrometer (Bruker) and a Varian Unity plus 600 (^{1}H NMR 600 MHz, ^{13}C NMR 151 MHz)

spectrometer. Chemical shifts (δ) were reported in parts per million (ppm) against the reference compound tetramethylsilane (TMS) and calculated using the solvent residual peak of the deuterated solvent. ESI-MS spectra were recorded with a Micro Tof (BRUKER DALTONICS).

The following UPLC-UV/MS system was used: precolumn: Zorbax Eclipse Plus-C18 (2.1 x 12.5 mm, 5 µm particle size); column: Zorbax SB-C18 (2.1 x 50 mm, 1.8 µm particle size); degasser: 1260 HiP (G4225A) (AGILENT); pump: 1260 Bin Pump (G1212B) (AGILENT); autosampler: 1260 HiP ALS (G1367E) (AGILENT); column oven: 1290 TCC (G1316C) (AGILENT); MS-detector: 6120 Quadrulpol LC/MS (G1978B) (AGILENT); MS source: multimode source; precolumn: Chiralpak® HSA HPLC Guard Column (2.0 x 10 mm, 5 µm particle size); column: Chiralpak® HSA HPLC Column (2.0 x 50 mm, 5 µm particle size); temperature: 25 °C; solvent: ammonium acetate (50 mM, pH 7.4) bidist. water:*i*-PrOH 96:4; isocratic. The following HPLC systems were used: Method A: pump: WellChrom K-1800 (KNAUER); UV detector: Smartline 2500 (KNAUER, λ = 254 nm); column: Nucleosil 100-5 C-18, 4.6 mm × 250 mm; solvent A: water with 0.1% (v/v) trifluoroacetic acid; solvent B: acetonitrile with 0.1% (v/v) trifluoroacetic acid; flow rate: 1.5 mL/min; gradient elution: (A%): 0 – 4 min: 90% , 4 – 33 min: gradient from 90% to 30%, 33 – 43 min: 30%, 43 – 45 min: gradient from 30% to 0%, 45 – 50 min: 0%, 50 – 53 min: gradient from 50% to 53%. Method B: The following HPLC was used to determine the enantiomeric purity of pyrazol derivates **19** and **22**. pump: L-7150 (MERCK-HITACHI); UV/vis detector: L-7400 (MERCK-HITACHI); autosampler: L-7200 (LaChrom, MERCK-HITACHI); column: Chiralpack® AS 5 µm (DIACEL), 4.6 mm × 250 mm; solvent: *i*-hexane:ethanol:methanol 70:15:15 + 0.1% formic acid; flow rate: 1.0 mL/min; isocratic. Method C1: The reaction mixtures of radiolabeled compounds were purified and separated with semipreparative radio-HPLC at room temperature. Pumps: K

500 and K 501 (KNAUER); UV detector: K 2000 (KNAUER, λ = 254 nm); γ-Detector: NaI(TI) Scintibloc 51 SP51 (CRISMATEC); column: ACE 126-2510, 10 mm × 250 mm; solvent A: water with 0.1% (v/v) trifluoroacetic acid; solvent B: acetonitrile with 0.1% (v/v) trifluoroacetic acid; flow rate: 5.5 mL; gradient elution: (A%): 0 – 45 min: gradient from 80% to 30%, 45 – 50 min: 30%, 50 – 55 min: 30% to 80%. Method C2: gradient elution: (A%): 0 – 30 min: gradient from 80% to 50%, 30 – 45 min: gradient 50% to 30%, 45 – 55 min: 30% to 80%. Method D: pump: Smartline 1000 (KNAUER); UV detector: Smartline 2500 (KNAUER, λ = 254 nm); γ-Detector: GabiStar (RAYTEST ISOTOPENMESSGERÄTE GMBH); column: Nucleosil 100-5 C-18, 4 mm × 250 mm, solvent: A: water with 0.1% (v/v) trifluoroacetic acid; solvent B: acetonitrile with 0.1% (v/v) trifluoroacetic acid; flow rate: 1.0 mL/min, gradient elution: (A%): 0 – 15 min: gradient from 90% to 0%, 15 – 18 min: 0%, 18– 20 min: 0% to 90%. Purity of the target compounds was ≥ 97% determined by HPLC (HPLC methods are specified in the individual sections of the compounds).

Synthetic procedures

General Procedure for Suzuki-Miyaura Coupling Method A (General Procedure A)

Pinacol boronic ester **15** or *ent*-**15** (1 - 3 eq), brominated heteroaromatic compounds (1 - 3 eq) and K_2CO_3 (2.0 - 6.3 eq) were added to DME/H_2O (7:1) and Ar was bubbled through the mixture for 30 min to remove O_2. $Pd(PPh_3)_2Cl_2$ (0.1 eq) was added and the reaction mixture was stirred at 80 °C under Ar atmosphere for 5 - 24 h. After cooling to room temperature, brine (0.5 x DME/H_2O mL) was added and the reaction mixture was extracted with ethyl acetate (0.5 x brine mL), the combined organic layers were dried ($MgSO_4$), filtered and concentrated *in vacuo*. The crude product was purified by column chromatography or automatic flash column chromatography.

General procedure for Suzuki-Miyaura Coupling Method B (General Procedure B)

Pinacol boronic ester **15** (1. eq), brominated heteroaromatic compounds (1.5 eq) and K_2CO_3 (2.0 eq) were dissolved in DME/H_2O (1.6 - 3 mL, 7:1) in a microwave vial and Ar was bubbled through for 10 s. $Pd(PPh_3)_2Cl_2$ (0.1 eq) was added and the reaction mixture was heated in a microwave apparatus at 100 °C, 150 W for 20-60 min. After cooling to room temperature, brine (10 mL) was added and the reaction mixture was extracted with ethyl acetate (3 x 5 mL), the combined organic layers were dried ($MgSO_4$), filtered and concentrated *in vacuo*. The residue was purified by automatic flash column chromatography.

General procedure for deprotection of *tert*-butyl esters with KSF clay (General Procedure C)

tert-Butyl ester (0.05 - 18.63 mmol) was dissolved in acetonitrile (5 - 45 mL) and KSF clay (0.27 - 3.73 g) was added. The reaction mixture was stirred for 3.5 - 24 h under reflux. After filtration, the filtrate was concentrated *in vacuo*. The crude product was purified by column chromatography or automatic flash column chromatography.

General procedure for fluorination with DAST (General Procedure D)

DAST (3.1 eq) was added to an ice cooled solution of alcohol (1 eq) in toluene (3-5 mL) under Ar atmosphere and the reaction mixture was stirred at room temperature overnight. Water (10 mL) was added and the mixture was extracted with ethyl acetate (3 x 5 mL) and washed with brine (5 mL). The combined organic layers were dried ($MgSO_4$), filtered and concentrated *in vacuo.* The crude product was purified by column chromatography or automatic flash column chromatography.

***tert*-Butyl [(8-azidodibenzo[b,d]furan-3-yl)sulfonyl]-*(S)*-valinate (2)**

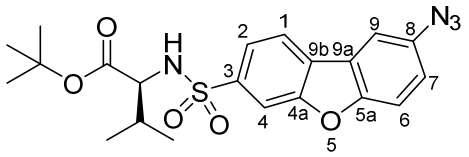

A mixture of arylbromide **1** (300 mg, 0.62 mmol), NaN_3 (81 mg, 1.25 mmol), sodium ascorbate (6 mg, 0.03 mmol), CuI (14 mg, 0.07 mmol) and DMEDA (13 µL, 0.13 mmol) in EtOH/H_2O (15 mL, (7:3)) was degassed and stirred for 30 min under reflux. After cooling to room temperature the reaction mixture was extracted with CH_2Cl_2 (3 x 5 mL), the combined organic layers were dried ($MgSO_4$), filtered and concentrated *in vacuo*. The crude product was purified by column chromatography (cyclohexane:ethyl acetate (6:1)) to give **2** (260 mg, 0.58 mmol, 94%) as brown solid; mp = 133-135 °C. TLC: R_f = 0.39, cyclohexane:ethyl acetate (4:1). ^{1}H NMR (400 MHz, $CDCl_3$): δ [ppm] = 8.06 (dd, $^5J_{H,H}$ = 0.4 Hz, $^4J_{H,H}$ = 1.5 Hz, 1H, 4-$CH_{dibenzofuran}$), 8.02 (dd, $^5J_{H,H}$ = 0.4 Hz, $^3J_{H,H}$ = 8.2 Hz, 1H, 1-$CH_{dibenzofuran}$), 7.85 (dd, $^4J_{H,H}$ = 1.6 Hz, $^3J_{H,H}$ = 8.2 Hz, 1H, 2-$CH_{dibenzofuran}$), 7.62 (dd, $^5J_{H,H}$ = 0.4 Hz, $^4J_{H,H}$ = 2.4 Hz, 1H, 9-$CH_{dibenzofuran}$), 7.60 (dd, $^5J_{H,H}$ = 0.4 Hz, $^3J_{H,H}$ = 8.8 Hz, 1H, 6-$CH_{dibenzofuran}$), 7.21 (dd, $^4J_{H,H}$ = 2.4 Hz, $^3J_{H,H}$ = 8.8 Hz, 1H, 7-$CH_{dibenzofuran}$), 5.27 (d, $^3J_{H,H}$ = 9.9 Hz, 1H, N*H*), 3.72 (dd, $^3J_{H,H}$ = 4.5 Hz, $^3J_{H,H}$ = 9.9 Hz, 1H, C*H*NH), 2.07 (dsept, $^3J_{H,H}$ = 4.7 Hz, $^3J_{H,H}$ = 6.8 Hz, 1H, C*H*(CH_3)$_2$), 1.11 (s, 9H, C(C*H*$_3$)$_3$), 1.01 (d, $^3J_{H,H}$ = 6,8 Hz, 3H, CH(C*H*$_3$)$_2$), 0.86 (d, $^3J_{H,H}$ = 6,9 Hz, 3H, CH(C*H*$_3$)$_2$). ^{13}C NMR (101 MHz, $CDCl_3$):δ [ppm] = 170.4 (1C, *C*OO^{t}Bu), 156.1 (1C, C-4a$_{dibenzofuran}$), 154.9 (1C, C-5a$_{dibenzofuran}$), 139.2 (1C, C-3$_{dibenzofuran}$), 136.2 (1C, C-8$_{dibenzofuran}$), 127.7 (1C, C-9b$_{dibenzofuran}$), 124.2 (1C, C-9a$_{dibenzofuran}$), 122.2 (1C, C-2$_{dibenzofuran}$), 121.5 (1C, C-1$_{dibenzofuran}$), 120.5 (1C, C-7$_{dibenzofuran}$), 113.5 (1C, C-6$_{dibenzofuran}$), 111.8 (1C, C-4$_{dibenzofuran}$), 111.3 (1C, C-9$_{dibenzofuran}$), 82.6 (1C, *C*(CH_3)$_3$), 61.6 (1C, *C*HNH), 31.9 (1C, *C*H(CH_3)$_2$), 27.7 (3C, C(*C*H$_3$)$_3$), 19.3 (1C, CH(*C*H$_3$)$_2$), 17.3 (1C, CH(*C*H$_3$)$_2$)). HRMS (ESI$^+$): *m / z* = [M+Na]$^+$ calcd for $C_{21}H_{24}N_4O_5SNa$ 467.1360, found 467.1358.

***tert*-Butyl ({8-[4-(3-fluoropropyl)-1,2,3-triazol-1-yl]dibenzo[*b,d*]furan-3-yl)sulfonyl)-*(S)*-valinate (3)**

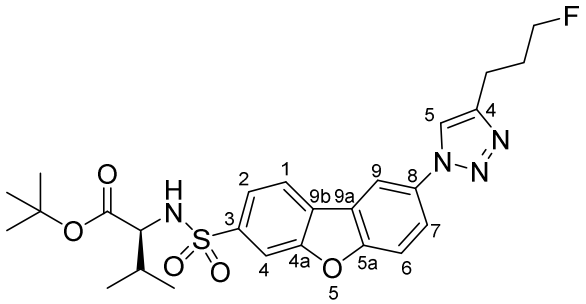

Azide **2** (190 mg, 0.45 mmol), 5-fluoropent-1-yne (560 mg, 6.5 mmol), sodium ascorbat (89 mg, 0.45 mmol) and $CuSO_4 \cdot 5\ H_2O$ (112 mg, 0.45 mmol) were mixed with DMF/H_2O (9 mL, 6:3) and the reaction mixture was stirred at room temperature overnight. Water (20 mL) was added and the reaction mixture was extracted with CH_2Cl_2 (3x 5 mL), the combined organic layers were washed with brine (5 mL), dried ($MgSO_4$), filtered and concentrated *in vacuo*. The crude product was purified by automatic flash column chromatography (column: Reveleris® Silica 12 g, flow rate 30 mL/min, ethyl acetate:cyclohexane (3% → 34% ethyl acetate, 25 min) to yield **3** (110 mg, 20 mmol, 49%) as colorless solid; mp: 175-179 °C. TLC: R_f = 0.53 cyclohexane:ethyl acetate (1:1). ^{1}H NMR (600 MHz, $CDCl_3$): δ [ppm] = 8.37 (d, $^4J_{H,H}$ = 2.2 Hz, 1H, 9-CH $_{dibenzofuran}$), 8.10 (d, $^4J_{H,H}$ = 1.4 Hz, 1H, 4-CH $_{dibenzofuran}$), 8.07 (d, $^3J_{H,H}$ = 8.2 Hz, 1H, 1-CH $_{dibenzofuran}$), 7.88 (dd, $^4J_{H,H}$ = 1.1 Hz, $^3J_{H,H}$ = 8.2 Hz, 1H, 2-CH $_{dibenzofuran}$), 7.87 (dd, $^4J_{H,H}$ = 2.1 Hz, $^3J_{H,H}$ = 8.6 Hz, 1H, 7-CH $_{dibenzofuran}$), 7.87 (s, 1H, 5-CH$_{triazole}$), 7.74 (d, $^3J_{H,H}$ = 8.8 Hz, 1H, 6-CH $_{dibenzofuran}$), 5.27 (d, $^3J_{H,H}$ = 10.5 Hz, 1H, N*H*), 4.57 (dt, $^2J_{H,F}$ = 47.2 Hz, $^3J_{H,H}$ = 5.8 Hz, 2H, $CH_2CH_2CH_2F$), 3.72 (dd, $^3J_{H,H}$ = 9.8 Hz, $^3J_{H,H}$ = 4.5 Hz, 1H, C*H*NH), 2.99 (t, $^3J_{H,H}$ = 7.5 Hz, 2H, $CH_2CH_2CH_2F$), 2.20 (dtt, $^3J_{H,F}$ = 26.1 Hz, $^3J_{H,H}$ = 5.9 Hz, $^3J_{H,H}$ = 7.3 Hz, 2H, $CH_2CH_2CH_2F$), 2.07 (dsept, $^3J_{H,H}$ = 6.8 Hz, $^3J_{H,H}$ = 5.1 Hz, 1H, $CH(CH_3)_2$), 1.11 (s, 9H, $C(CH_3)_3$), 1.01 (d, $^3J_{H,H}$ = 6,8 Hz, 3H, $CH(CH_3)_2$), 0.86 (d, $^3J_{H,H}$ = 6,8 Hz, 3H, $CH(CH_3)_2$).^{13}C NMR (151 MHz, $CDCl_3$):δ

[ppm] = 170.3 (1C, *C*OO^{t}Bu), 156.8 (1C, C-5a $_{dibenzofuran}$), 156.2 (1C, C-4a $_{dibenzofuran}$), 148.0 (1C, C-4$_{triazole}$), 139.7 (1C, C-3 $_{dibenzofuran}$), 133.5 (1C, C-8 $_{dibenzofuran}$), 127.6 (1C, C-9b $_{dibenzofuran}$), 124.00 (1C, C-9a $_{dibenzofuran}$), 122.4 (1C, C-7 $_{dibenzofuran}$), 121.7 (1C, C-2 $_{dibenzofuran}$), 121.6 (1C, C-1 $_{dibenzofuran}$), 120.0 (1C, C-5$_{triazole}$), 114.1 (1C, C-9 $_{dibenzofuran}$), 113.3 (1C, C-6 $_{dibenzofuran}$), 111.9 (1C, C-4 $_{dibenzofuran}$), 83.2 (d, $^2J_{C,F}$ = 165.2 Hz, 1C, $CH_2CH_2CH_2F$), 82.6 (1C, $C(CH_3)_3$), 61.6 (1C, *C*HNH), 31.8 (1C, $CH(CH_3)_2$), 30.1 (d, $^3J_{C,F}$ = 29.9 Hz, 1C, $CH_2CH_2CH_2F$), 27.7 (3C, $C(CH_3)_3$), 21.6 (d, $^4J_{C,F}$ = 5.5 Hz, 1C, $CH_2CH_2CH_2F$), 19.2 (1C, $CH(CH_3)_2$), 17.2 (1C, $CH(CH_3)_2$). ^{19}F NMR (282 MHz, $CDCl_3$): δ [ppm] = -220.66 (tt, 1F, $^2J_{H,F}$ = 47.2 Hz, $^3J_{H,F}$ = 26.1 Hz). HRMS (ESI$^+$): *m / z* = $[M+Na]^+$ calcd for $C_{26}H_{31}N_4FO_5SNa$ 553.1891, found 553.1892.

{[8-(4-(3-Fluoropropyl)-1*H*-1,2,3-triazol-1-yl)dibenzo[b,d]furan-3-yl]sulfonyl}-(*S*)-valine (4)

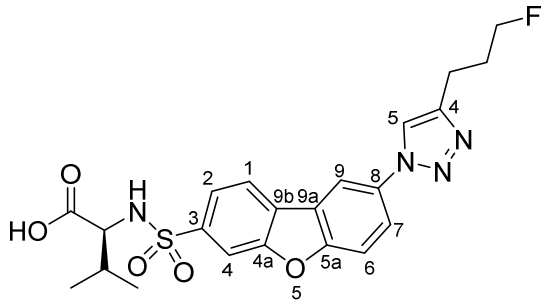

General procedure C: *tert*-Butyl ester **3** (110 mg, 0.21 mmol), KSF clay (207 mg) 5 h reflux in acetonitrile (10 mL). Purification by column chromatography ($CHCl_3$:MeOH (18:1)) gave **4** (80 mg, 0.17 mmol, 81%) as colorless solid; mp: 233-235 °C. TLC: R_f = 0.22 $CHCl_3$:MeOH (18:1). HPLC (Method A): t_R = 30.18 min, purity 99.5%. ^{1}H NMR (400 MHz, CD_2Cl_2/CD_3OD (1:1)): δ [ppm] = 8.31 (d, $^4J_{H,H}$ = 2.1 Hz, 1H, 4-CH $_{dibenzofuran}$), 8.18 (s, 1H, 5-CH$_{triazole}$), 7.98 (d, $^3J_{H,H}$ = 8.2 Hz, 1H, 6-CH $_{dibenzofuran}$), 7.95 (d, $^4J_{H,H}$ = 0.8 Hz, 1H, 9-CH $_{dibenzofuran}$), 7.84 (dd, $^3J_{H,H}$ = 8.9 Hz, $^4J_{H,H}$ = 2.3 Hz, 1H, 2-CH $_{dibenzofuran}$), 7.75 (dd, $^3J_{H,H}$ = 8.2 Hz, $^4J_{H,H}$ = 1.6 Hz, 1H, 7-CH $_{dibenzofuran}$), 7.60 (d, $^3J_{H,H}$ = 8.9 Hz, 1H, 1-CH $_{dibenzofuran}$), 4.45 (dt, $^2J_{H,F}$ = 47.3 Hz, $^3J_{H,H}$ = 5.8 Hz, 2H, $CH_2CH_2CH_2F$), 3.50 (d, $^3J_{H,H}$ = 4.4 Hz, 1H, C*H*NH), 2.87-2.82 (m, 2H, $CH_2CH_2CH_2F$),

2.15-2.06 (m, 2H, $CH_2CH_2CH_2F$), 2.06-1.94 (m, 1H, $CH(CH_3)_2$), 0.85 (d, $^3J_{H,H}$ = 6.8 Hz, 3H, $CH(CH_3)_2$), 0.75 (d, $^3J_{H,H}$ = 6.8 Hz, 3H $CH(CH_3)_2$). ^{13}C NMR (101 MHz, CD_2Cl_2:CD_3OD (1:1)): δ [ppm] = 177.7 (1C, *C*OOH), 157.6 (1C, C-4a $_{dibenzofuran}$), 156.9 (1C, C-5a $_{dibenzofuran}$), 148.7 (1C, C-4$_{triazole}$), 141.3 (1C, C-8 $_{dibenzofuran}$), 134.1 (1C, C-3 $_{dibenzofuran}$), 127.9 (1C, C-9b $_{dibenzofuran}$), 124.8 (1C, C-9a $_{dibenzofuran}$), 123.0 (1C, C-7 $_{dibenzofuran}$), 122.4 (1C, C-6 $_{dibenzofuran}$), 122.2 (1C, C-2 $_{dibenzofuran}$), 121.6 (1C, C-5$_{triazole}$), 114.5 (1C, C-4 $_{dibenzofuran}$), 113.7 (1C, C-1 $_{dibenzofuran}$), 112.1 (1C, C-9 $_{dibenzofuran}$), 83.6 (d, $^2J_{C,F}$ = 164.5 Hz, 1C, $CH_2CH_2CH_2F$), 63.9 (1C, *C*HNH), 32.3 (1C, $CH(CH_3)_2$), 30.8 (d, $^3J_{C,F}$ = 19.8 Hz, 1C, $CH_2CH_2CH_2F$), 21.9 (1C, $CH_2CH_2CH_2F$), 19.8 (1C, $CH(CH_3)_2$), 17.7 (1C, $CH(CH_3)_2$). ^{19}F NMR (282 MHz, CD_2Cl_2:CD_3OD (1:1)): δ [ppm] = -217.49 (tt, 1F, $^2J_{H,F}$ = 47.2 Hz, $^3J_{H,F}$ = 25.7 Hz). HRMS (ESI$^+$): m/z = $[M+Na]^+$ calcd for $C_{22}H_{23}FN_4O_5SNa$ 497.1265, found 497.1259.

[(8-Azidodibenzo[*b,d*]furan-3-yl)sulfonyl]-*(S)*-valine (5)

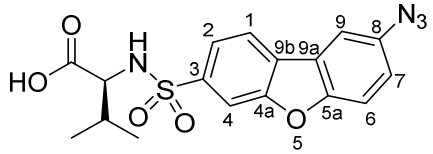

General procedure C: *tert*-Butyl ester **2** (120 mg, 0.27 mmol), KSF clay (270 mg) after 5 h reflux in acetonitrile (15 mL). Purification by column chromatography ($CHCl_3$:MeOH (18:1)) gave **5** (83 mg, 0.21 mmol, 79%) as brown solid; mp: 170-172 °C. TLC: R_f = 0.35, $CHCl_3$:MeOH (18:1). HPLC (Method A): t_R = 29.8 min, purity 98%. ^{1}H NMR (400 MHz, DMSO-d_6): δ [ppm] = 8.29 (d, $^3J_{H,H}$ = 8.1 Hz, 1H, 1-CH $_{dibenzofuran}$), 8.05 (d, $^4J_{H,H}$ = 1.4 Hz, 1H, 4-CH $_{dibenzofuran}$), 8.02 (d, $^4J_{H,H}$ = 2.5 Hz, 1H, 9-CH $_{dibenzofuran}$), 7.81 (dd, $^4J_{H,H}$ = 1.6 Hz, $^3J_{H,H}$ = 8.2 Hz, 1H, 2-CH $_{dibenzofuran}$), 7.75 (d, $^3J_{H,H}$ = 8.8 Hz, 1H, 6-CH $_{dibenzofuran}$), 7.29 (dd, $^4J_{H,H}$ = 2.5 Hz, $^3J_{H,H}$ = 8.8 Hz, 1H, 7-CH $_{dibenzofuran}$), 3.36 (d, $^3J_{H,H}$ = 4.4 Hz, 1H, C*H*NH), 2.06-1.98 (m, 1H, $CH(CH_3)_2$), 0.83 (d, $^3J_{H,H}$ = 6,8 Hz, 3H, $CH(CH_3)_2$), 0.75 (d, $^3J_{H,H}$ = 6,8 Hz, 3H, $CH(CH_3)_2$). ^{13}C NMR (101 MHz,

DMSO-d_6): δ [ppm] = 173.1 (1C, *C*OOH), 155.2 (1C, C-4a $_{dibenzofuran}$), 153.9 (1C, C-5a $_{dibenzofuran}$), 140.6 (1C, C-3 $_{dibenzofuran}$), 135.4 (1C, C-8 $_{dibenzofuran}$), 126.3 (1C, C-9b $_{dibenzofuran}$), 123.9 (1C, C-9a $_{dibenzofuran}$), 122.1 (1C, C-1$_{dibenzofuran}$), 121.8 (1C, C-2 $_{dibenzofuran}$), 120.3 (1C, C-7 $_{dibenzofuran}$), 113.3 (1C, C-6 $_{dibenzofuran}$), 112.1 (1C, C-9 $_{dibenzofuran}$), 110.6 (1C, C-4 $_{dibenzofuran}$), 62.5 (1C, *C*HNH), 30.9 (1C, *C*H(CH$_3$)$_2$), 19.4 (1C, CH(*C*H$_3$)$_2$), 17.8 (1C, CH(*C*H$_3$)$_2$). HRMS (ESI$^+$): m/z = [M+Na]$^+$ calcd for $C_{17}H_{16}N_4O_5SNa$ 411.0739, found 411.0734.

***tert*-Butyl ({8-[(trimethylsilyl)ethynyl]dibenzo[*b,d*]furan-3-yl}sulfonyl)-*(S)*-valinate (6)**

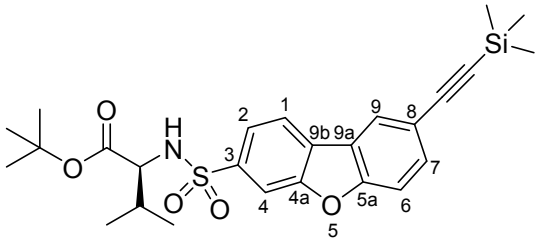

Compound **1** (300 mg, 0.62 mmol), ethynyltrimethylsilane (0.15 mL, 0.95 mmol) and NEt$_3$ (0.45 mL, 3.11 mmol) were dissolved in DMF (30 mL) and Ar was bubbled through the solution for 30 min. Pd(PPh$_3$)$_2$Cl$_2$ (42 mg, 0.06 mmol) and CuI (12 mg, 0.06 mmol) were added and the reaction mixture was strirred at 65 °C under Ar atmosphere for 16 h. After cooling to room temperature, water (30 mL) was added and the reaction mixture was extracted with CH$_2$Cl$_2$ (3x 10 mL), the combined organic layers were dried (MgSO$_4$), filtered and concentrated *in vacuo*. The crude product was purified by column chromatography (cyclohexane:ethyl acetate (9:1)) to obtain **6** (211 mg, 0.42 mmol, 68%) as colorless solid; mp: 120-122 °C. TLC: R_f = 0.25 cyclohexane:ethyl acetate (9:1). ^{1}H NMR (400 MHz, CDCl$_3$): δ [ppm] = 8.13 (dd, $^5J_{H,H}$ = 0.7 Hz, $^4J_{H,H}$ = 1.7 Hz, 1H, 9-CH $_{dibenzofuran}$), 8.06 (dd, $^5J_{H,H}$ = 0.6 Hz, $^4J_{H,H}$ = 1.6 Hz, 1H, 4-CH $_{dibenzofuran}$), 8.01 (dd, $^5J_{H,H}$ = 0.6 Hz, $^3J_{H,H}$ = 8.2 Hz, 1H, 1-CH $_{dibenzofuran}$), 7.85 (dd, $^4J_{H,H}$ = 1.6 Hz, $^3J_{H,H}$ = 8.2 Hz, 1H, 2-CH $_{dibenzofuran}$), 7.66 (dd, $^4J_{H,H}$ = 1.7 Hz, $^3J_{H,H}$ = 8.6 Hz, 1H, 7-CH $_{dibenzofuran}$), 7.55 (dd, $^5J_{H,H}$ = 0.7 Hz, $^3J_{H,H}$ = 8.6 Hz, 1H, 6-CH $_{dibenzofuran}$), 5.22 (d, $^3J_{H,H}$ = 10.1 Hz, 1H, N*H*), 3.70 (dd,

$^3J_{H,H}$ = 4.5 Hz, $^3J_{H,H}$ = 9.9 Hz, 1H, C*H*NH), 2.06 (dsept, $^3J_{H,H}$ = 4.5 Hz, $^3J_{H,H}$ = 6.8 Hz, 1H, C*H*$(CH_3)_2$), 1.08 (s, 9H, C(C*H*$_3)_3$), 1.02 (d, $^3J_{H,H}$ = 6.7 Hz, 3H, CH(C*H*$_3)_2$), 0.86 (d, $^3J_{H,H}$ = 6.8 Hz, 3H, CH(C*H*$_3)_2$), 0.29 (s, 9H, Si(C*H*$_3)_3$). ^{13}C NMR (101 MHz, $CDCl_3$): δ [ppm] = 170.4 (1C, *C*OO^{t}Bu), 157.3 (1C, C-5a $_{dibenzofuran}$), 155.8 (1C, C-4a $_{dibenzofuran}$), 139.0 (1C, C-3 $_{dibenzofuran}$), 133.0 (1C, C-7 $_{dibenzofuran}$), 127.8 (1C, C-9b $_{dibenzofuran}$), 125.5 (1C, C-9 $_{dibenzofuran}$), 123.1 (1C, C-9a $_{dibenzofuran}$), 122.4 (1C, C-2 $_{dibenzofuran}$), 121.4 (1C, C-1 $_{dibenzofuran}$), 118.9 (1C, C-8 $_{dibenzofuran}$), 112.8 (1C, C-6 $_{dibenzofuran}$), 111.8 (1C, C-4 $_{dibenzofuran}$), 104.6 (1C, *C*CSi$(CH_3)_3$), 94.3 (1C, C*C*Si$(CH_3)_3$), 82.8 (1C, *C*$(CH_3)_3$), 61.6 (1C, *C*HNH), 31.9 (1C, *C*H$(CH_3)_2$) 27.7 (3C, C(*C*H$_3)_3$), 19.3 (1C, CH(*C*H$_3)_2$), 17.3 (1C, CH(*C*H$_3)_2$), 0.18 (3C, Si(*C*H$_3)_3$). HRMS (ESI$^+$): *m / z* = $[M+Na]^+$ calcd for $C_{26}H_{33}NO_5SSiNa$ 522.1738, found 522.1741.

***tert*-Butyl [(8-ethynyldibenzo[*b,d*]furan-3-yl)sulfonyl]-*(S)*-valinate (7)**

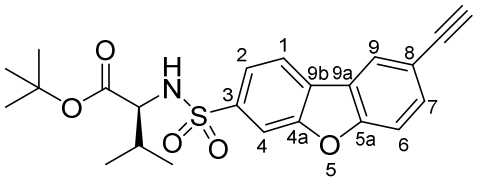

Compound **6** (170 mg, 0.34 mmol) was dissolved in MeOH (8 mL) and K_2CO_3 (103 mg, 0.75 mmol) was added. The reaction mixture was stirred at room temperature overnight. The solvent was removed *in vacuo* and ethyl acetate (10 mL) was added to the residue. The mixture was washed with water (2 x 5 mL) and brine (1 x 5 mL). The combined organic layers were dried ($MgSO_4$), filtered and concentrated *in vacuo*. The crude product was purified by automatic flash column chromatography (column: Reveleris® Silica 12 g, flow rate 30 mL/min, ethyl acetate:cyclohexane (3% → 18% ethyl acetate, 15 min)) to give **7** (137 mg, 0.32 mmol, 94%) as colorless solid; mp: 148-150 °C. TLC: R_f = 0.24 cyclohexane:ethyl acetate (8:1). ^{1}H NMR (400 MHz, $CDCl_3$): δ [ppm] = 8.11 (d, $^4J_{H,H}$ = 1.6 Hz, 1H, 9-CH $_{dibenzofuran}$), 8.04 (d, $^4J_{H,H}$ = 1.5 Hz, 1H,

4-CH $_{dibenzofuran}$), 7.99 (d, $^3J_{H,H}$ = 8.2 Hz, 1H, 1-CH $_{dibenzofuran}$), 7.84 (dd, $^4J_{H,H}$ = 1.5 Hz, $^3J_{H,H}$ = 8.2 Hz, 1H, 2-CH $_{dibenzofuran}$), 7.65 (dd, $^4J_{H,H}$ = 1.6 Hz, $^3J_{H,H}$ = 8.6 Hz, 1H, 7-CH $_{dibenzofuran}$), 7.54 (d, $^3J_{H,H}$ = 8.6 Hz, 1 H, 6-CH $_{dibenzofuran}$), 5.25 (d, $^3J_{H,H}$ = 9.9 Hz, 1H, N*H*), 3.69 (dd, $^3J_{H,H}$ = 4.6 Hz, $^3J_{H,H}$ = 9.9 Hz, 1H, C*H*NH), 3.10 (s, 1 H, CC*H*), 2.04 (dsept, $^3J_{H,H}$ = 4.6 Hz, $^3J_{H,H}$ = 6.9 Hz, 1H, C*H*$(CH_3)_2$), 1.07 (s, 9H, C(C*H*$_3$)$_3$), 0.99 (d, $^3J_{H,H}$ = 6.8 Hz, 3H, CH(C*H*$_3$)$_2$), 0.83 (d, $^3J_{H,H}$ = 6.9 Hz, 3H, CH(C*H*$_3$)$_2$). ^{13}C NMR (101 MHz, $CDCl_3$):δ [ppm] = 170.4 (1C, *C*OO^{t}Bu), 157.4 (1C, C-5a $_{dibenzofuran}$), 155.8 (1C, C-4a $_{dibenzofuran}$), 139.1 (1C, C-3 $_{dibenzofuran}$), 133.1 (1C, C-7 $_{dibenzofuran}$), 127.7 (1C, C-9b $_{dibenzofuran}$), 125.6 (1C, C-9 $_{dibenzofuran}$), 123.2 (1C, C-9a $_{dibenzofuran}$), 122.4 (1C, C-2 $_{dibenzofuran}$), 121.4 (1C, C-1 $_{dibenzofuran}$), 117.8 (1C, C-8 $_{dibenzofuran}$), 112.5 (1C, C-6 $_{dibenzofuran}$), 111.8 (1C, C-4 $_{dibenzofuran}$), 83.2 (1C, *C*CH), 82.6 (1C, *C*$(CH_3)_3$), 77.3 (1C, C*C*H), 61.6 (1C, *C*HNH), 31.9 (1C, *C*H$(CH_3)_2$) 27.7 (3C, C(*C*H$_3$)$_3$), 19.3 (1C, CH(*C*H$_3$)$_2$), 17.3 (1C, CH(*C*H$_3$)$_2$). HRMS (ESI$^+$): m/z = $[M+Na]^+$ calcd for $C_{23}H_{25}NO_5SNa$ 450.1246, found 450.1340.

***tert*-Butyl ({8-[1-(2-fluoroethyl)-1,2,3-triazol-4-yl]dibenzo[*b,d*]furan-3-yl}sulfonyl)-*(S)*-valinate (8)**

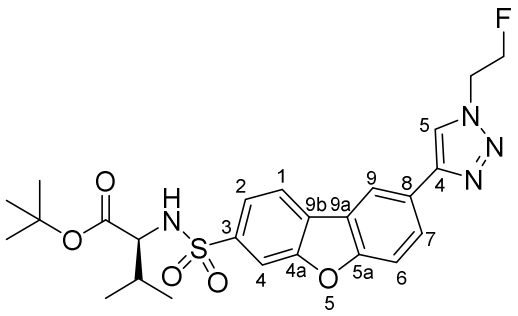

Sodium azide (219 mg, 3.37 mmol) was added to a solution of 2-fluoroethyl 4-methylbenzenesulfonate (245 mg, 1.12 mmol) in DMF (5 mL) and the reaction mixture was stirred at room temperature overnight. After full conversion (reaction control: GC/MS), the mixture was filtered into another flask with compound **7** (143 mg, 0.33 mmol). The filter was washed with DMF (5 mL). Sodium ascorbat (464 mg, 2.34 mmol) and $CuSO_4 \cdot 5\ H_2O$ (418 mg,

1.67 mmol) were added and the reaction mixture was stirred at room temperature for 4 h. Water (15 mL) was added and the reaction mixture was extracted with ethyl acetate (3 x 5 mL), the combined organic layers were dried ($MgSO_4$), filtered and concentrated *in vacuo*. The crude product was purified by automatic flash column chromatography (column: Reveleris® Silica 12 g, flow rate 30 mL/min, ethyl acetate:cyclohexane (16% → 52% ethyl acetate, 20 min)) to give **8** (141 mg, 0.27 mmol, 83%) as colorless solid; mp: 167-169 °C. TLC: R_f = 0.23 cyclohexane:ethyl acetate (1:1). ^{1}H NMR (400 MHz, CD_2Cl_2:CD_3OD (1:1)): δ [ppm] = 8.38 (d, $^4J_{H,H}$ = 1.7 Hz, 1H, 9-CH $_{dibenzofuran}$), 8.19 (s, 1H, 5-CH$_{triazole}$), 8.05 (d, $^3J_{H,H}$ = 8.2 Hz, 1H, 1-CH $_{dibenzofuran}$), 7.95 (d, $^4J_{H,H}$ = 1.2 Hz, 1H, 4-CH $_{dibenzofuran}$), 7.89 (dd, $^4J_{H,H}$ = 1.8 Hz, $^3J_{H,H}$ = 8.6 Hz, 1H, 7-CH $_{dibenzofuran}$), 7.75 (dd, $^4J_{H,H}$ = 1.6 Hz, $^3J_{H,H}$ = 8.1 Hz, 1H, 2-CH $_{dibenzofuran}$), 7.56 (dd, $^3J_{H,H}$ = 8.6 Hz, 1H, 6-CH $_{dibenzofuran}$), 4.86 (dt, $^2J_{H,F}$ = 46.6 Hz, $^3J_{H,H}$ = 4.8 Hz, 2H, CH_2CH_2F), 4.71 (dt, $^3J_{H,F}$ = 26.8 Hz, $^3J_{H,H}$ = 4.5 Hz, 2H, CH_2CH_2F), 3.58 (d, $^3J_{H,H}$ = 5.5 Hz, 1H, C*H*NH), 2.04-1.96 (m, 1H, C*H*$(CH_3)_2$), 0.99 (s, 9H, C(C*H*$_3$)$_3$), 0.88 (d, $^3J_{H,H}$ = 6.8 Hz, 3H, CH(C*H*$_3$)$_2$), 0.79 (d, $^3J_{H,H}$ = 6.8 Hz, 3H, CH(C*H*$_3$)$_2$). ^{13}C NMR (101 MHz, CD_2Cl_2:CD_3OD (1:1)): δ [ppm] = 171.8 (1C, *C*OO^{t}Bu), 158.6 (1C, C-5a $_{dibenzofuran}$), 157.0 (1C, C-4a $_{dibenzofuran}$), 148.8 (1C, C-4$_{triazole}$), 140.8 (1C, C-3 $_{dibenzofuran}$), 129.2 (1C, C-9b $_{dibenzofuran}$), 128.0 (1C, C-7 $_{dibenzofuran}$) 127.5 (1C, C-8 $_{dibenzofuran}$), 124.7 (1C, C-9a $_{dibenzofuran}$), 123.2 (1C, C-2 $_{dibenzofuran}$), 122.8 (1C, C-5$_{triazole}$), 122.6 (1C, C-1 $_{dibenzofuran}$), 119.8 (1C, C-9 $_{dibenzofuran}$), 113.6 (1C, C-6 $_{dibenzofuran}$), 112.4 (1C, C-4 $_{dibenzofuran}$), 83.2 (1C, *C*$(CH_3)_3$), 83.0 (d, $^2J_{C,F}$ = 171.1 Hz, 1C, CH_2*C*H_2F), 63.3 (d, *C*HNH), 50.3 (d, $^3J_{C,F}$ = 52.2 Hz, 1C, *C*H_2CH_2F), 32.8 (1C, *C*H$(CH_3)_2$), 28.3 (3C, C(*C*H$_3$)$_3$), 20.0 (1C, CH(*C*H$_3$)$_2$), 18.3 (1C, CH(*C*H$_3$)$_2$).^{19}F NMR (282 MHz, CD_2Cl_2:CD_3OD (1:1)):δ [ppm] = -221.80 (tt, 1F, $^2J_{H,F}$ = 47.0 Hz, $^3J_{H,F}$ = 26.8 Hz). HRMS (ESI$^+$): *m / z* = $[M+Na]^+$ calcd for $C_{25}H_{29}FN_4O_5SNa$ 539.1735, found 539.1729.

{[8-(1-(2-Fluoroethyl)-1,2,3-triazol-4-yl)dibenzo[*b,d*]furan-3-yl]sulfonyl}-*(S)*-valine (9)

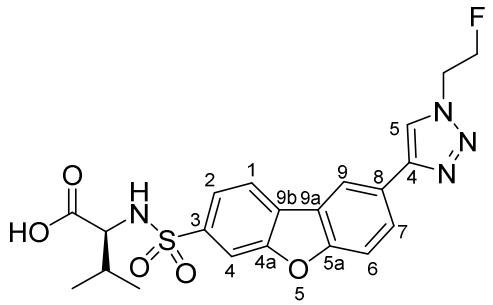

General procedure C: *tert*-Butyl ester **8** (149 mg, 0.29 mmol), KSF clay (60 mg) was heated to reflux for 6 h in acetonitrile (3 mL). Purification by column chromatography ($CHCl_3$:MeOH (18:1)) to yield **9** (107 mg, 0.23 mmol, 80%) as colorless solid; mp: 212-214 °C. TLC: R_f = 0.26 $CHCl_3$:MeOH (18:1). HPLC (Method A): t_R = 30.18 min, purity 98.2%. ^{1}H NMR (400 MHz, DMSO-d_6): δ [ppm] = 8.76 (d, $^4J_{H,H}$ = 1.5 Hz, 1H, 9-CH $_{dibenzofuran}$), 8.70 (s, 1H, 5-CH$_{triazole}$), 8.37 (d, $^3J_{H,H}$ = 8.1 Hz, 1H, 1-CH $_{dibenzofuran}$), 8.09 (dd, $^4J_{H,H}$ = 1.7 Hz, $^3J_{H,H}$ = 8.7 Hz, 1H, 7-CH $_{dibenzofuran}$), 8.08-8.09 (m, 1H, 4-CH $_{dibenzofuran}$), 7.86 (d, $^3J_{H,H}$ = 8.8 Hz, 1H, 6-CH $_{dibenzofuran}$), 7.83 (dd, $^4J_{H,H}$ = 1.5 Hz, $^3J_{H,H}$ = 8.2 Hz, 1H, 2-CH $_{dibenzofuran}$), 4.90 (dt, $^2J_{H,F}$ = 46.7 Hz, $^3J_{H,H}$ = 4.9 Hz, 2H, CH_2CH_2F), 4.81 (dt, $^3J_{H,F}$ = 27.8 Hz, $^3J_{H,H}$ = 4.9 Hz, 2H, CH_2CH_2F), 3.38 (d, $^3J_{H,H}$ = 4.1 Hz, 1H, *C*HNH), 2.04-1.96 (m, 1H, $CH(CH_3)_2$), 0.85 (d, $^3J_{H,H}$ = 6.8 Hz, 3H, $CH(CH_3)_2$), 0.78 (d, $^3J_{H,H}$ = 6.8 Hz, 3H, $CH(CH_3)_2$). ^{13}C NMR (101 MHz, DMSO-d_6): δ [ppm] = 172.1 (1C, *C*OOH), 156.3 (1C, C-5a $_{dibenzofuran}$), 154.9 (1C, C-4a $_{dibenzofuran}$), 146.3 (1C, C-4$_{triazole}$), 140.2 (1C, C-3 $_{dibenzofuran}$), 126.8 (1C, C-9b $_{dibenzofuran}$), 126.7 (1C, C-7 $_{dibenzofuran}$), 126.5 (1C, C-8 $_{dibenzofuran}$), 123.1 (1C, C-9a $_{dibenzofuran}$), 121.9 (1C, C-1 $_{dibenzofuran}$), 121.8 (2C, C-2, C-5$^t_{riazole}$), 118.5 (1C, C-9 $_{dibenzofuran}$), 112.5 (1C, C-6 $_{dibenzofuran}$), 110.5 (1C, C-4 $_{dibenzofuran}$), 82.0 (d, $^2J_{C,F}$ = 167.9 Hz, 1C, CH_2CH_2F), 62.2 (1C, *C*HNH), 50.3 (d, $^3J_{C,F}$ = 19.5 Hz, 1C, CH_2CH_2F), 30.7 (1C, $CH(CH_3)_2$), 19.4 (1C, $CH(CH_3)_2$), 17.8 (1C, $CH(CH_3)_2$). ^{19}F NMR (300 MHz, DMSO-d_6):δ [ppm] = -221.28

(tt, 1F, $^2J_{H,F}$ = 46.9 Hz, $^3J_{H,F}$ = 28.2 Hz). HRMS (ESI$^+$): m/z = [M+Na]$^+$ calcd for $C_{21}H_{21}FN_4O_5SNa$ 483.1109, found 483.1103.

[(8-Ethynyldibenzo[*b,d*]furan-3-yl)sulfonyl]-*(S)*-valine (10)

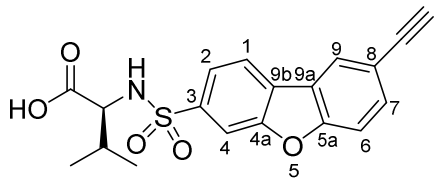

General procedure C: *tert*-Butyl ester **7** (60 mg, 0.14 mmol), KSF clay (140 mg), 5 h reflux in acetonitrile (8 mL). Purification by column chromatography ($CHCl_3$:MeOH (18:1)) to obtain **10** (37 mg, 0.1 mmol, 71%) as colorless solid; mp: 212-214 °C. TLC: R_f = 0.31 $CHCl_3$:MeOH (18:1). HPLC (Method D): t_R = 12.75 min, purity 99.6%. ^{1}H NMR (400 MHz, ^{1}H NMR (400 MHz, CD_2Cl_2 /CD_3OD (1:1)): δ [ppm] = 8.15 (d, $^4J_{H,H}$ = 1.2 Hz, 1H, 9-CH $_{dibenzofuran}$), 8.06 (d, $^3J_{H,H}$ = 8.2 Hz, 1H, 1-CH $_{dibenzofuran}$), 8.05 (d, $^4J_{H,H}$ = 1.0 Hz, 1H, 4-CH) $_{dibenzofuran}$, 7.83 (dd, $^4J_{H,H}$ = 1.3 Hz, $^3J_{H,H}$ = 8.6 Hz, 1H, 2-CH $_{dibenzofuran}$), 7.64 (dd, $^4J_{H,H}$ = 1.4 Hz, $^3J_{H,H}$ = 8.5 Hz, 1H, 7-CH $_{dibenzofuran}$), 7.56 (d, $^3J_{H,H}$ = 8.5 Hz, 1H, 6-CH $_{dibenzofuran}$), 3.72 (d, $^3J_{H,H}$ = 5.0 Hz, 1H, C*H*NH), 3.27 (s, 1H, CC*H*), 2.04 (dsept, $^3J_{H,H}$ = 5.0 Hz, $^3J_{H,H}$ = 6.8 Hz, 1H, C*H*$(CH_3)_2$), 0.92 (d, $^3J_{H,H}$ = 6.8 Hz, 3H, CH(CH_3)$_2$), 0.84 (d, $^3J_{H,H}$ = 6.8 Hz, 3H, CH(CH_3)$_2$). ^{13}C NMR (101 MHz, CD_2Cl_2/CD_3OD (1:1)): δ [ppm] = 173.6 (1C, *C*OOH), 158.0 (1C, C-5a $_{dibenzofuran}$), 156.3 (1C, 4a $_{dibenzofuran}$) ,140.2 (1C, C-3 $_{dibenzofuran}$), 133.4 (1C, C-7 $_{dibenzofuran}$), 128.0 (1C, C-9b $_{dibenzofuran}$), 126.0 (1C, C-9 $_{dibenzofuran}$), 123.9 (1C, C-9a $_{dibenzofuran}$), 122.7 (1C, C-2 $_{dibenzofuran}$), 122.0 (1C, C-1 $_{dibenzofuran}$), 118.3 (1C, C-8 $_{dibenzofuran}$), 112.8 (1C, C-6 $_{dibenzofuran}$), 111.8 (1C, C-4 $_{dibenzofuran}$), 83.5 (1C, C*C*H), 77.6 (1C, *C*CH), 62.0 (1C, *C*HNH), 32.0 (1C, *C*H$(CH_3)_2$), 19.4 (1C, CH(*C*H_3)$_2$), 17.6 (1C, CH(*C*H_3)$_2$). HRMS (ESI$^+$): m/z = [M+Na]$^+$ calcd for $C_{19}H_{17}NO_5SNa$ 394.0720, found 394.0714.

***tert*-Butyl ({8-[1-(2-fluoroethyl)pyrazol-4-yl]dibenzo[*b,d*]furan-3-yl}sulfonyl)-(*S*)-valinate (18)**

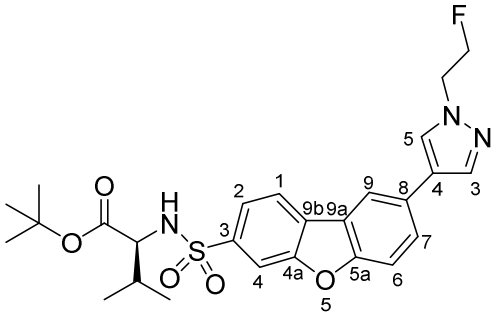

General Procedure A: Boronate **15** (66 mg, 0.13 mmol), 4-bromo-1-(2-fluoroethyl)pyrazole (**14**, 72 mg, 0.37 mmol), K_2CO_3 (94 mg, 0.68 mmol) and $Pd(PPh_3)_2Cl_2$ (9 mg, 0.01 mmol) in DME/H_2O (8 mL, 7:1) was stirred for 3 h at reflux. The crude product was purified by automatic flash column chromatography (column: Reveleris® Silica 12 g, flow rate 30 mL/min, ethyl acetate:cyclohexane (2% → 61% ethyl acetate, 30 min) to yield **18** (30 mg, 0.06 mmol, 47%) as colorless solid; mp: 166-168 °C. TLC: R_f = 0.15 cyclohexane:ethyl acetate (3:1). HPLC (Method C1): t_R = 39.50 min, purity 99.8%. ^{1}H NMR (400 MHz, $CDCl_3$): δ [ppm] = 8.03-8.01 (m, 3H, 1-CH, 4-CH, 9-CH $_{dibenzofuran}$), 7.87 (s, 1H, 3-CH$_{pyrazole}$), 7.82 (dd, $^3J_{H,H}$ = 8.2 Hz, $^4J_{H,H}$ = 1.5 Hz, 1H, 2-CH $_{dibenzofuran}$), 7.79 (s, 1H, 5-CH$_{pyrazole}$), 7.64 (dd, $^3J_{H,H}$ = 8.6 Hz, $^4J_{H,H}$ = 1.7 Hz, 1H, 7-CH $_{dibenzofuran}$), 7.58 (d, $^3J_{H,H}$ = 8.6 Hz, 1H, 6-CH $_{dibenzofuran}$), 5.26 (d, $^3J_{H,H}$ = 10.5 Hz, 1H, N*H*), 4.81 (dt, $^2J_{H,F}$ = 47.0 Hz $^3J_{H,H}$ = 4.7 Hz, 2H, CH_2F), 4.48 (dt, $^3J_{H,F}$ = 27.1 Hz, $^3J_{H,H}$ = 4.7 Hz, 2H, CH_2CH$_2$F), 3.70 (dd, $^3J_{H,H}$ = 9.9 Hz, $^3J_{H,H}$ = 4.5 Hz, 1H, C*H*NH), 2.03 (dsept, $^3J_{H,H}$ = 6.8 Hz, $^3J_{H,H}$ = 4.7 Hz, 1H, C*H*(CH$_3$)$_2$), 1.08 (s, 9H, C(CH$_3$)$_3$), 0.99 (d, $^3J_{H,H}$ = 6.8 Hz, 3H, CH(CH_3)$_2$), 0.84 (d, $^3J_{H,H}$ = 6.8 Hz, 3H, CH(CH_3)$_2$). ^{13}C NMR (101 MHz, $CDCl_3$): δ [ppm] = 170.4 (1C, *C*OO^{t}Bu), 156.5 (1C, C-5a $_{dibenzofuran}$), 155.7 (1C, C-4a $_{dibenzofuran}$), 138.6 (1C, C-3 $_{dibenzofuran}$), 137.6 (1C, C-3$_{pyrazole}$), 128.7 (1C, C-8 $_{dibenzofuran}$), 128.6 (1C, C-9b $_{dibenzofuran}$), 127.3 (1C, C-5$_{pyrazole}$), 127.3 (1C, C-6 $_{dibenzofuran}$), 123.5 (1C, C-9a $_{dibenzofuran}$), 123.2 (1C, C-4$_{pyrazole}$), 122.0 (1C, C-2 $_{dibenzofuran}$), 121.2

(1C, C-1 $_{dibenzofuran}$), 118.2 (1C, C-9 $_{dibenzofuran}$), 112.6 (1C, C-7 $_{dibenzofuran}$), 111.6 (1C, C-4 $_{dibenzofuran}$), 82.6 (1C, $C(CH_3)_3$), 82.2 (d, $^1J_{C,F}$ = 171.7 Hz, CH_2F), 61.6 (1C, *C*HNH), 52.9 (d, $^2J_{C,F}$ = 20.1 Hz, CH_2CH_2F), 31.9 (1C, $CH(CH_3)_2$), 27.7 (3C, $C(CH_3)_3$), 19.2 (1C, $CH(CH_3)_2$), 17.2 (1C, $CH(CH_3)_2$). ^{19}F NMR (282 MHz, $CDCl_3$): δ [ppm] = -221.66 (tt, 1F, $^2J_{H,F}$ = 46.9 Hz, $^3J_{H,F}$ = 27.2 Hz). HRMS (ESI$^+$): *m / z* = $[M+Na]^+$ calcd for $C_{26}H_{30}FN_3O_5SNa$ 538.1782, found 538.1796.

({8-[1-(2-Fluoroethyl)pyrazol-4-yl]dibenzo[*b,d*]furan-3-yl}sulfonyl)-(*S*)-valine (19)

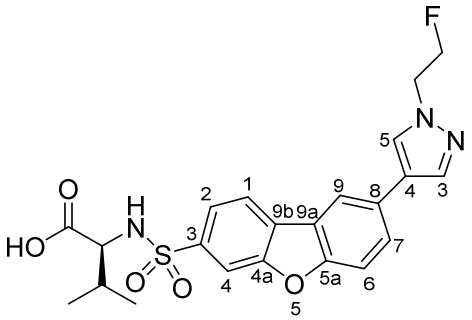

General procedure C: *tert*-Butyl ester **18** (28 mg, 0.05 mmol), KSF clay (54 mg) was stirred at 5 h at reflux in acetonitrile (5 mL). Purification by column chromatography ($CHCl_3$:MeOH (18:1)) to give **19** (20 mg, 0.04 mmol, 80%) as colorless solid; mp: 233-235 °C (decomposition). TLC: R_f = 0.38 $CHCl_3$:MeOH (18:1). HPLC (Method D): t_R = 11.70 min, purity 99.8%. Chiral HPLC (Method B): t_R = 8.49 min, enantiomeric purity >99.9%. ^{1}H NMR (400 MHz, DMSO-d_6): δ [ppm] = 12.15 (s, COO*H*), 8.49 (s, 1H, 9-CH $_{dibenzofuran}$), 8.30 (d, $^3J_{H,H}$ = 7.9 Hz, 1H, 1-CH $_{dibenzofuran}$), 8.30 (s, 1H, 5-$CH_{pyrazole}$), 8.18 (d, $^3J_{H,H}$ = 9.2 Hz, 1H, N*H*), 8.05 (m, 2H, 4-CH, 3-$CH_{pyrazole}$),7.85 (dd, $^3J_{H,H}$= 8.4 Hz, $^4J_{H,H}$ = 1.3 Hz, 1H, 7-CH $_{dibenzofuran}$), 7.83 (dd, $^3J_{H,H}$= 8.0 Hz, $^4J_{H,H}$ = 1.3 Hz, 1H, 2-CH $_{dibenzofuran}$), 7.78 (d, $^3J_{H,H}$= 8.6 Hz, 1H, 6-CH $_{dibenzofuran}$), 4.83 (dt, $^2J_{H,F}$ = 47.3 Hz, $^3J_{H,H}$ = 4.4 Hz, 2H, CH_2F), 4.49 (dt, $^3J_{H,F}$ = 27.9 Hz, $^3J_{H,H}$ = 4.3 Hz, 2H, CH_2CH_2F), 3.61 (dd, $^3J_{H,H}$ = 9.6 Hz, $^3J_{H,H}$ = 5.7 Hz, 1H, C*H*NH), 1.99-1.91 (m, 1H, $CH(CH_3)_2$), 0.84 (d, $^3J_{H,H}$ = 6.5 Hz, 3H, $CH(CH_3)_2$), 0.80 (d, $^3J_{H,H}$ = 6.6 Hz, 3H, $CH(CH_3)_2$). ^{13}C NMR (400 MHz, DMSO-d_6) δ [ppm] = 172.0 (1C, *C*OOH), 155.3 (1C, C-5a $_{dibenzofuran}$), 154.8 (1C, C-4a $_{dibenzofuran}$), 140.1 (1C,

C-3 $_{dibenzofuran}$), 136.7 (1C, C-3$_{pyrazole}$), 128.5 (1C, C-8 $_{dibenzofuran}$), 127.8 (1C, C-5$_{pyrazole}$), 127.1 (1C, C-9b $_{dibenzofuran}$), 126.4 (1C, C-7 $_{dibenzofuran}$), 123.1 (1C, C-4$_{pyrazole}$), 121.8 (1C, C-9a $_{dibenzofuran}$), 121.6 (1C, C-2 $_{dibenzofuran}$), 121.5 (1C, C-1 $_{dibenzofuran}$), 118.0 (1C, C-9 $_{dibenzofuran}$), 112.3 (1C, C-6 $_{dibenzofuran}$), 110.3 (1C, C-4 $_{dibenzofuran}$), 82.1 (d, $^{1}J_{C,F}$ = 167.8 Hz, 1C, CH_2F), 61.3 (1C, C*H*NH), 52.0 (d, $^{2}J_{C,F}$ = 19.7 Hz, 1C, *C*H_2CH$_2$F), 30.4 (1C, C*H*(CH$_3$)$_2$), 19.0 (1C, CH(C*H*$_3$)$_2$), 17.8 (1C, CH(C*H*$_3$)$_2$). ^{19}F NMR (282 MHz, DMSO-d_6): δ [ppm] = -221.57 (tt, 1F, $^{2}J_{H,F}$ = 47.2 Hz, $^{3}J_{H,F}$ = 27.9 Hz). HRMS (ESI$^+$): *m / z* = [M+Na]$^+$ calcd for $C_{22}H_{22}FN_3O_5SNa$ 482.1156, found 482.1157.

***tert*-Butyl ({8-[5-(2-hydroxyethyl)thiophen-2-yl]dibenzo[*b,d*]furan-3-yl}sulfonyl)-(*S*)-valinate (32)**

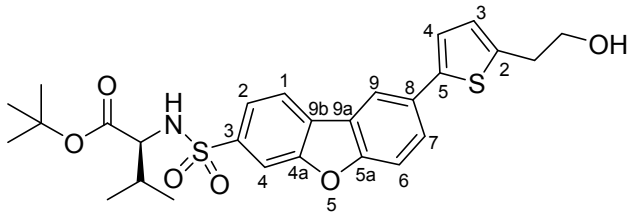

General Procedure B: Boronate **15** (50 mg, 0.09 mmol), 2-(5-bromothiophen-2-yl)ethan-1-ol (29 mg, 0.14 mmol), K_2CO_3 (26 mg, 0.19 mmol) and Pd(PPh$_3$)$_2$Cl$_2$ (7 mg, 0.01 mmol) in DME/H_2O (1.6 mL, 7:1) after 20 min. The residue product was purified by automatic flash column chromatography (column: Reveleris® Silica 4 g, flow rate 15 mL/min, ethyl acetate:cyclohexane: ethyl acetate (10% → 61% ethyl acetate, 20 min) to obtain **32** (20 mg, 0.04 mmol, 40%) as colorless solid; mp: 166-168 °C. TLC: R_f = 0.20 cyclohexane:ethyl acetate (2:1). ^{1}H NMR (400 MHz, $CDCl_3$): δ [ppm] = 8.12 (d, $^{4}J_{H,H}$ = 1.8 Hz, 1H, 9-CH $_{dibenzofuran}$), 8.05 (d, $^{3}J_{H,H}$ = 7.7 Hz, 1H, 1-CH $_{dibenzofuran}$), 8.05 (d, $^{4}J_{H,H}$ = 1.5 Hz, 1H, 4-CH $_{dibenzofuran}$), 7.85 (dd, $^{3}J_{H,H}$ = 8.2 Hz, $^{4}J_{H,H}$ = 1.5 Hz, 1H, 2-CH $_{dibenzofuran}$), 7.75 (dd, $^{3}J_{H,H}$ = 8.6 Hz, $^{4}J_{H,H}$ = 1.9 Hz, 1H, 7-CH $_{dibenzofuran}$), 7.60 (d, $^{3}J_{H,H}$ = 8.6 Hz, 1H, 6-CH $_{dibenzofuran}$), 7.21 (d, $^{3}J_{H,H}$ = 3.5 Hz, 1H, 3-CH$_{thiophene}$), 6.89 (d, $^{3}J_{H,H}$ = 3.5 Hz, 1H, 4-CH$_{thiophene}$), 5.23 (d, $^{3}J_{H,H}$ = 9.9 Hz, 1H, N*H*), 3.93 (t,

$^3J_{H,H}$ = 6.2 Hz, 2H, C*H*$_2$OH), 3.72 (dd, $^3J_{H,H}$ = 9.8, $^3J_{H,H}$ = 4.5 Hz, 1H, C*H*NH), 3.12 (t, $^3J_{H,H}$ = 6.3 Hz, 2H, C*H*$_2$CH$_2$OH), 2.06 (m, 1H, C*H*(CH$_3$)$_2$), 1.10 (s, 9H, C(C*H*$_3$)$_3$), 1.01 (d, $^3J_{H,H}$ = 6.8 Hz, 3H, CH(C*H*$_3$)$_2$), 0.86 (d, $^3J_{H,H}$ = 6.9 Hz, 3H, CH(C*H*$_3$)$_2$). ^{13}C NMR (101 MHz, CDCl$_3$): δ [ppm] = 170.4 (1C, *C*OO^{t}Bu), 156.9 (1C, C-5a $_{dibenzofuran}$), 155.8 (1C, C-4a $_{dibenzofuran}$) , 142.4 (1C, C-2$_{thiophene}$), 141.0 (1C, C-5$_{thiophene}$), 138.7 (1C, C-3 $_{dibenzofuran}$), 130.7 (1C, C-8 $_{dibenzofuran}$), 128.2 (1C, C-9b $_{dibenzofuran}$), 127.2 (1C, C-7 $_{dibenzofuran}$), 127.0 (1C, C-4$_{thiophene}$), 123.5 (1C, C-9a $_{dibenzofuran}$), 123.4 (1C, C-3$_{thiophene}$), 122.1 (1C, C-2 $_{dibenzofuran}$), 121.3 (1C, C-1 $_{dibenzofuran}$), 118.3 (1C, C-9 $_{dibenzofuran}$), 112.6 (1C, C-6 $_{dibenzofuran}$), 111.6 (1C, C-4 $_{dibenzofuran}$), 82.6 (1, *C*(CH$_3$)$_3$), 63.5 (1C, C*H*$_2$OH), 61.6 (1C, *C*HNH), 33.8 (1C, *C*H$_2$CH$_2$OH), 31.8 (1C, *C*H(CH$_3$)$_2$), 27.7 (3C, C(*C*H$_3$)$_3$), 19.2 (1C, CH(*C*H$_3$)$_2$), 17.2 (1C, CH(*C*H$_3$)$_2$). HRMS (ESI$^+$): *m / z* = [M+Na]$^+$ calcd for C$_{27}$H$_{31}$NO$_6$S$_2$Na 552.1490, found 552.1480.

***tert*-Butyl ({8-[5-(2-fluoroethyl)thiophen-2-yl]dibenzo[*b,d*]furan-3-yl}sulfonyl)-(*S*)-valinate (33)**

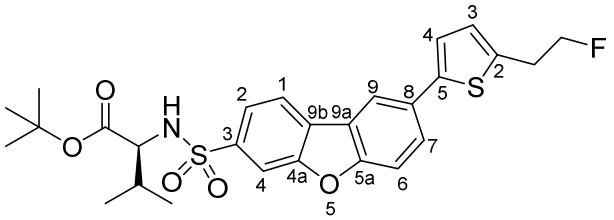

General Procedure D: Alcohol **32** (69 mg, 0.13 mmol) and DAST (53 µL, 0.40 mmol) in toluene (3 mL) overnight at room temperature. Purification by automatic flash column chromatography (column: Reveleris® Silica 12 g, flow rate 28 mL/min, ethyl acetate:cyclohexane (10% → 50% ethyl acetate, 20 min) to give **33** (57 mg, 0.11 mmol, 83%) as colorless solid; mp: 147-149 °C. TLC: R$_f$ = 0.32 cyclohexane:ethyl acetate (4:1). ^{1}H NMR (400 MHz, CDCl$_3$): δ [ppm] = 8.13 (d, $^4J_{H,H}$ = 1.4 Hz, 1H, 9-CH $_{dibenzofuran}$), 8.05 (d, $^3J_{H,H}$ = 7.8 Hz, 1H, 1-CH $_{dibenzofuran}$), 8.06 (d, $^4J_{H,H}$ = 1.5 Hz, 1H, 4-CH $_{dibenzofuran}$), 7.86 (dd, $^3J_{H,H}$ = 8.2 Hz, $^4J_{H,H}$ = 1.5 Hz, 1H, 2-CH $_{dibenzofuran}$), 7.76

(dd, $^3J_{H,H}$ = 8.6 Hz, $^4J_{H,H}$ = 1.9 Hz, 1H, 7-CH $_{dibenzofuran}$), 7.61 (d, $^3J_{H,H}$ = 8.6 Hz, 1H, 6-CH $_{dibenzofuran}$), 7.21 (d, $^3J_{H,H}$ = 3.6 Hz, 1H, 4-CH$_{thiophene}$), 6.90 (d, $^3J_{H,H}$ = 3.6 Hz, 1H, 3-CH$_{thiophene}$), 5.22 (d, $^3J_{H,H}$ = 9.9 Hz, 1H, CHN*H*), 4.69 (dt, $^2J_{H,F}$ = 46.9 Hz, $^3J_{H,H}$ = 6.2 Hz, 2H, CH_2F), 3.72 (dd, $^3J_{H,H}$ = 9.9 Hz, $^3J_{H,H}$ = 4.5 Hz, 1H, C*H*NH), 3.26 (dt, $^3J_{H,F}$ = 23.3 Hz, $^3J_{H,H}$ = 6.5 Hz, 2H, CH_2CH$_2$F), 2.07 (dsept, $^3J_{H,H}$ = 6.8 Hz, $^3J_{H,H}$ = 4.7 Hz, 1H, C*H*(CH$_3$)$_2$), 1.11 (s, 9H, C(CH_3)$_3$), 1.01 (d, $^3J_{H,H}$ = 6.8 Hz, 3H, CH(CH_3)$_2$), 0.86 (d, $^3J_{H,H}$ = 6.9 Hz, 3H, CH(CH_3)$_2$). ^{13}C NMR (101 MHz, CDCl$_3$): δ [ppm] = 170.4 (1C, COO^{t}Bu), 157.0 (1C, C-5a $_{dibenzofuran}$), 155.8 (1C, C-4a $_{dibenzofuran}$), 142.6 (1C, C-4$_{thiophene}$), 139.1 (d, $^3J_{C,F}$ = 5.5 Hz, 1C, C-5$_{thiophene}$), 138.7 (1C, C-3 $_{dibenzofuran}$), 130.6 (1C, C-8 $_{dibenzofuran}$), 128.2 (1C, C-9a $_{dibenzofuran}$), 127.2 (1C, C-7 $_{dibenzofuran}$), 127.1 (1C, C-3^{thiophene}), 123.5 (1C, C-9b $_{dibenzofuran}$), 123.4 (1C, C-4$_{thiophene}$), 122.1 (1C, C-2 $_{dibenzofuran}$), 121.3 (1C, C-1 $_{dibenzofuran}$), 118.4 (1C, C-9 $_{dibenzofuran}$), 112.6 (1C, C-6 $_{dibenzofuran}$), 111.6 (1C, C-4 $_{dibenzofuran}$), 83.7 (d, $^1J_{C,F}$ = 170.3 Hz, 1C, *C*H$_2$F), 82.6 (1C, *C*(CH$_3$)$_3$), 61.6 (1C, *C*HNH), 31.9 (1C, *C*H(CH$_3$)$_2$), 31.6 (d, $^2J_{C,F}$ = 21.6 Hz, 1C, *C*H$_2$CH$_2$F), 27.7 (3C, C(*C*H$_3$)$_3$), 19.2 (1C, CH(*C*H$_3$)$_2$), 17.2 (1C, CH(*C*H$_3$)$_2$). ^{19}F NMR (282 MHz, CDCl$_3$): δ [ppm] = -215.14 (tt, 1F, $^2J_{H,F}$ = 47.0 Hz, $^3J_{H,F}$ = 24.0 Hz). HRMS (ESI$^+$): m/z = [M+Na]$^+$ calcd for $C_{27}H_{30}FNO_5S_2Na$. 554.1442, found 554.1448.

({8-[5-(2-Fluoroethyl)thiophen-2-yl)dibenzo[*b,d*]furan-3-yl]sulfonyl}-(*S*)-valine (34)

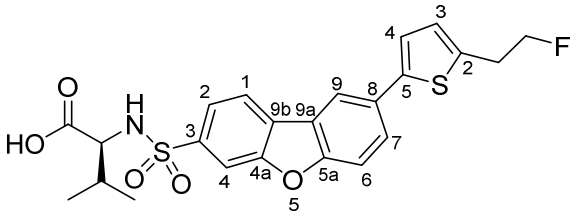

General Procedure C: *tert*-Butyl ester **33** (54 mg, 0.10 mmol), KSF clay (100 mg) 4 h reflux in acetonitrile (5 mL). Purification by column chromatography (CHCl$_3$:MeOH (18:1)) to obtain **34** (26 mg, 0.05 mmol, 54%) as colorless solid; mp: 183-185 °C. TLC: R_f = 0.35 CHCl$_3$:MeOH

(40:1). HPLC (Method D): t_R = 14.95 min, purity 99.8%. ^{1}H NMR (400 MHz, DMSO-d_6): δ [ppm] = 8.51 (d, $^4J_{H,H}$ = 1.5 Hz, 1H, 9-CH $_{dibenzofuran}$), 8.40 (d, $^3J_{H,H}$ = 8.4 Hz, 1H, 1-CH $_{dibenzofuran}$), 8.17 (s, 1H, N*H*), 8.06 (d, $^4J_{H,H}$ = 1.1 Hz, 1H, 4-CH $_{dibenzofuran}$), 7.86 (dd, $^3J_{H,H}$ = 8.7 Hz, $^4J_{H,H}$ = 2.0 Hz, 1H, 7-CH $_{dibenzofuran}$), 7.83 (dd, $^3J_{H,H}$ = 8.2 Hz, $^4J_{H,H}$ = 1.5 Hz, 1H, 2-CH $_{dibenzofuran}$), 7.81 (d, $^3J_{H,H}$ = 8.7 Hz, 1H, 6-CH $_{dibenzofuran}$), 7.45 (d, $^3J_{H,H}$ = 3.6 Hz, 1H, 4-CH$_{thiophene}$), 7.00 (d, $^3J_{H,H}$ = 3.6 Hz, 1H, 3-CH$_{thiophene}$), 4.68 (dt, $^2J_{H,F}$ = 47.2 Hz, $^3J_{H,H}$ = 5.9 Hz, 2H, C*H*$_2$F), 3.60 (d, $^3J_{H,H}$ = 4.8 Hz, 1H, C*H*NH), 3.24 (dt, $^4J_{H,F}$ 26.4 Hz, $^3J_{H,H}$ = 5.9 Hz, 2H, *C*H$_2$CH$_2$F), 2.01-1.89 (m, 1H, C*H*(CH$_3$)$_2$), 0.83 (d, $^3J_{H,H}$ = 6.8 Hz, 3H, CH(C*H*$_3$)$_2$), 0.80 (d, $^3J_{H,H}$ = 6.8 Hz, 3H, CH(C*H*$_3$)$_2$). ^{13}C NMR (101 MHz, DMSO-d_6): δ [ppm] = 172.1 (1C, *C*OOH), 156.0 (1C, C-5a $_{dibenzofuran}$), 154.9 (1C, C-4a $_{dibenzofuran}$), 141.5 (1C, C-2 $_{thiophene}$), 140.4 (1C, C-3 $_{dibenzofuran}$), 139.4 (1C, $^3J_{C,F}$ = 4.4 Hz, C-5$_{thiophene}$), 130.0 (1C, C-8 $_{dibenzofuran}$), 127.4 (1C, C-4$_{thiophene}$), 126.9 (1C, C-9b $_{dibenzofuran}$), 126.5 (1C, C-7 $_{dibenzofuran}$), 123.7 (1C, C-3$_{thiophene}$), 123.3 (1C, C-9a $_{dibenzofuran}$), 122.0 (1C, C-1 $_{dibenzofuran}$), 121.7 (1C, C-2 $_{dibenzofuran}$), 118.4 (1C, C-9 $_{dibenzofuran}$), 112.6 (1C, C-6 $_{dibenzofuran}$), 110.4 (1C, C-4 $_{dibenzofuran}$), 83.7 (1C, $^1J_{C,F}$ = 166.4 Hz, *C*H$_2$F), 61.4 (1C, *C*HNH), 30.7 (1C, $^2J_{C,F}$ = 20.8 Hz, *C*H$_2$CH$_2$F), 30.5 (1C, *C*H(CH$_3$)$_2$), 19.1 (1C, CH(*C*H$_3$)$_2$), 17.9 (1C, CH(*C*H$_3$)$_2$). ^{19}F NMR (282 MHz, DMSO-d_6): δ [ppm] = -214.52 (tt, 1F, $^2J_{H,F}$ = 47.2 Hz, $^3J_{H,F}$ = 26.4 Hz). HRMS (ESI$^+$): *m / z* = [M+Na]$^+$ calcd for $C_{23}H_{22}FNO_5S_2Na$ 498.0816, found 498.0879.

***In vitro* MMP assays**

The inhibition potencies of compounds **4**, **5**, **9**, **10**, **12a-b**, **17**, **19**, *ent*-**19**, **25**, **28**, **31** and **34** against activated MMP-2, -8, -9, -12 and -13 were measured following the protocol of Huang *et al.*.[54] Additionally inhibitors **4** and **9** were tested against MMP-1, -3 and -7. Here the synthetic compounds (7-methoxycoumarin-4-yl)acetyl-Pro-Leu-Gly-Leu-(3-(2,4-dinitrophenyl)-L-2,3-diaminopropionyl)Ala-Arg-NH$_2$ (R&D Systems) and (7-methoxycoumarin-4-yl)acetyl-Arg-Pro-

Lys-Pro-Val-Glu-Norval-Trp-Lys(2,4-dinitrophenyl)-NH_2 (R&D Systems) were used as fluorogenic substrates in the MMP-2, -3, -7, -8, -9, -12, -13 and MMP-1 assay, respectively. Different concentrations of the test compounds and the activated MMPs (each at 2 nM) were preincubated at 37 °C for 30 min in Tris buffer (50 mM), pH 7.5, containing NaCl (0.2 M), $CaCl_2$ (5 mM), $ZnSO_4$ (20 µM) and Brij 35 (0.05 %). To an aliquot of substrate (10 µL of 50 µM solution) the enzyme-inhibitor mixture (90 µL) was added. For monitoring the fluorescence changes a TriStar2 multimode reader LB 942 (BERTHOLD) with excitation and emission wavelengths of 340 and 405 nm was used. The reaction within the last 10 min were plotted as a function of inhibitor concentration. The IC_{50}-values were determined from the inhibition curves by nonlinear regression analysis using the Grace 5.1.8 software (Linux).

Determination of log$D_{7.4}$-values of non-radioactive compounds

In order to determine the log$D_{7.4}$ value, the shake flask method reported recently was utilized.[55] The following UPLC-UV/MS (AGILENT TECHNOLOGIES) system was used: LC-MS method: pump: 1260 Bin Pump (G1212B); MS-Detector: 6120 Quadrupole LC/MS (G1978B); precolumn: Zorbax Eclipse Plus-C18 5 µm, 2.1 mm x 12.5 mm; column: Zorbax SB-C18 1.8 µm, 2.1 mm x 50 mm; column oven: 1290 TCC (G1316C), 30 °C; degasser: 1260 HiP (G4225A); autosampler: 1260 HiP ALS (G1367E); MS source: multimode source; injection volume: 1 µL; solvent A: water:acetonitrile:HCO_2H 950:50:1; solvent B: acetonitrile:water:HCO_2H 950:50:1; flow rate: 0.3 mL/min; gradient elution: (A%): 0 – 2 min: gradient from 100% to 0%, 2 –3 min: 0%, 3 – 3.5 min: gradient from 0% to 100%, 3.5 – 8 min: 100%; MS parameter: Vaporizer temperature: 200 °C; drying gas: 12 L/min; nebulizer pressure: 35 psi; VCap: -4000 V; Fragmentor voltage and drying gas temperature were optimized for each compound by flow-injection analysis (FIA).

The six-port-valve (which normally switches between two columns) was used as a divert valve to protect the mass spectrometer from salts of the sample. After 1 min, the valve was switched from "waste" to "MS-source". At the end of a single run the valve was switched to "waste". The Multimode source was running only in the ESI mode. The calibration of the quadrupole was achieved by injection of APCI/APPI Tuning Mix (G2432A, AGILENT TECHNOLOGIES).

Experimental procedure: MOPS (372.5 mg, 8.9 mM) and MOPS sodium salt (513.4 mg, 11.1 mM) were dissolved in bidist. H_2O (200 mL) to prepare 20 mM MOPS buffer with pH 7.4. *n*-octanol and MOPS buffer were saturated with each other before the experiment by stirring a two-phase system for 24 h. The final concentration of DMSO was kept below 1 % in all samples. The log$D_{7.4}$ values were determined using three different volume ratios of buffer and *n*-octanol (750 µl and 750 µL (1/1), 500 µL and 1000 µL (1/2) and 1000 µL in 500 µL (2/1)). The 10 mM DMSO stock solution was diluted differently for each compound for being inside the linear range of the quadrupole detector. The diluted DMSO stock solution was added to the buffer, afterwards *n*-octanol was added. Those DMSO/buffer mixtures were pipetted into 1.5 mL safe lock tubes. Afterwards, the tubes where vortexed for 2 min and subsequently centrifuged at 20 °C with 16000 rpm for 10 min. An aliquot of the aqueous layer was analyzed with the above-mentioned LC-MS method. Each sample with one of the three ratios (buffer/*n*-octanol) was prepared in triplicate resulting in a total of n = 9 experiments. The calibration curve was prepared with MOPS buffer saturated with *n*-octanol to match the matrix of the samples, covering the concentration range.

Radiochemistry: General Methods

The radiosyntheses of the compounds **[^{18}F]4**, **[^{18}F]9** and **[^{18}F]19** were carried out semiautomated with a modified PET tracer radiosynthesiser TRACERLab FX_{FDG} and the TRACERLab Fx

software (GE Healthcare). The aqueous solutions of no-carrier-added [^{18}F]fluoride were produced by irradiation of 2.8 mL enriched [^{18}O]H_2O (97 %) on a RDS 111e cyclotron (CTI-Siemens) using 10 MeV proton beams to perform the ^{18}O(p,n)^{18}F nuclear reaction. Separation and purification of the reaction mixtures of the radiosynthezised compounds were performed on semipreparative radio-HPLC (Method C1 for **[^{18}F]4** and **[^{18}F]9**, Method C2 for **[^{18}F]19**). The radiochemical purities and molar activities were determined on an analytical radio-HPLC (Method D). The specified radiochemical yields given in this work are decay corrected (d. c.) after purification and formulation.

((8-(4-(3-[^{18}F]Fluoropropyl)-1,2,3-triazol-1-yl)dibenzo[b,d]furan-3-yl)sulfonyl)-(*S*)-valine ([^{18}F]4)

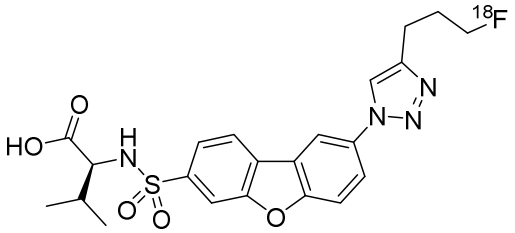

The aqueous [^{18}F]fluoride ions (1191 – 4990 MBq) from the cyclotron were passed through an anion exchange pre-conditioned cartridge (Sep-Pak® Light QMA, CO_3^{2-} as counter ion) in a computer controlled synthesizer. [^{18}F]Fluoride ions were eluted from the cartridge in the reactor with a solution of Kryptofix®2.2.2 (20 mg, 53 µmol, 4 eq) and K_2CO_3 (40 µL, 1 M, 40 µmol, 3 eq) in water (200 µL) and CH_3CN (800 µL). The aqueous K(K222)[^{18}F]F solution was carefully evaporated to dryness *in vacuo*. A solution of pent-4-yn-1-yl 4-methylbenzenesulfonate (20 mg, 84 µmol, 7 eq) in CH_3CN (500 µl) was added and the mixture was heated at 110 °C for 3 min. The produced 5-[^{18}F]fluoropent-1-yne was distilled from the reactor in a 5 mL flask containing DMF (300 µL, cooled to -10 °C) within 2 min. Then aqueous $CuSO_4 \cdot 5H_2O$-solution (0.4 M, 120 µL, 48 µmol, 4 eq), sodium ascorbate (16 mg, 81 µmol, 6 eq) in water (100 µL) and

precursor **5** (5.0 mg, 12.9 µmol, 1 eq) in DMF (100 µL) were added to the flask and the reaction mixture was stirred for 30 min at 40 °C. Then the mixture was passed through a Sep-Pak® Light cartridge filled with quartz wool. The cartridge was washed with DMF (200 µL). The eluate was diluted with water (500 µL). The resulting mixture was purified by semipreparative radio-HPLC (Method C1). The product fraction of **[^{18}F]4** (t_R = 24.4 min) was evaporated to dryness *in vacuo* and redissolved in water:EtOH (1 mL, 9:1). Triazole **[^{18}F]4** was obtained with a rcy of 37 ± 8 % (d. c., *n* = 6) and a rcp >99 % (t_R (analytical radio-HPLC, Method D) = 12.6 min) and a A_m in the range of 3 - 59 GBq/µmol in 126 ± 3 min.

((8-(1-(2-([^{18}F]Fluoro-ethyl)-1*H*-1,2,3-triazol-4-yl)dibenzo[b,d]furan-3-yl)sulfonyl)-(*S*)-valine ([^{18}F]9)

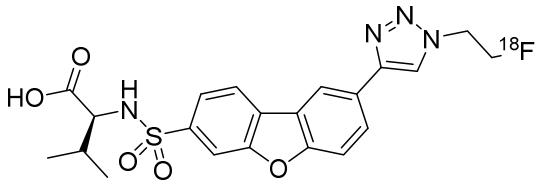

In a computer controlled synthesizer aqueous [^{18}F]fluoride ions (2392 – 4889 MBq) were passed through an anion exchange pre-conditioned cartridge (Sep-Pak® Light QMA, CO_3^{2-} as counter ion). [^{18}F]Fluoride ions were eluted from the cartridge with a solution of Kryptofix®2.2.2 (20 mg, 53 µmol, 4 eq) and K_2CO_3 (40 µL, 1 M, 40 µmol, 3 eq) in water (200 µL) and CH_3CN (800 µL) into the reactor. The aqueous solution was carefully evaporated to dryness *in vacuo*. A solution of 2-azidoethyl 4-methylbenzenesulfonate (20 mg, 83 µmol, 6 eq) in CH_3CN (500 µl) was added and the mixture was heated at 110 °C for 3 min. The formed 1-azido-2-[^{18}F]fluoroethane was distilled from the reactor in a 5 mL flask containing DMF (300 µL, cooled to -10 °C) within 2 min. Then aqueous $CuSO_4 \cdot 5H_2O$-solution (0.4 M, 120 µL, 48 µmol, 4 eq), sodium ascorbate (16 mg, 81 µmol, 6 eq) in water (100 µL) and precursor **10** (5.0 mg, 13.5 µmol, 1 eq) in DMF

(100 µL) were added to the flask. The reaction mixture was stirred for 30 min at 40 °C. Then, the mixture was passed through a Sep-Pak® Light cartridge filled with quartz wool. The cartridge was washed with DMF (200 µL). The eluate was diluted with water (500 µL). Purification was performed by semipreparative radio-HPLC (Method C1). The product fraction of **[^{18}F]9** (t_R = 21.4 min) was evaporated to dryness *in vacuo* and redissolved in water:EtOH (1 mL , 9:1). Triazole **[^{18}F]9** was obtained with a rcy of 43 ± 7 % (d. c., *n* = 6) and a rcp >99 % (t_R (analytical radio-HPLC, Method D) = 12.0 min) and a A_m in the range of 7 - 57 GBq/µmol in 140 ± 6 min.

((8-(1-(2-([^{18}F]Fluoroethyl)pyrazol-4-yl)dibenzo[b,d]furan-3-yl)sulfonyl)-(*S*)-valine ([^{18}F]19)

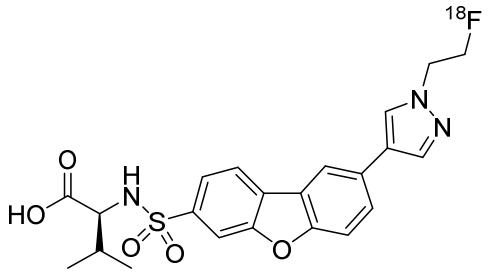

In a computer controlled synthesizer aqueous [^{18}F]fluoride ions (2392 - 4889 MBq) were passed through an anion exchange pre-conditioned cartridge (Sep-Pak® Light QMA, CO_3^{2-} as counter ion). [^{18}F]Fluoride ions were eluted from the cartridge with a solution of Kryptofix®2.2.2 (20 mg, 53 µmol, 7 eq) and K_2CO_3 (40 µL, 1 M, 40 µmol, 5 eq) in water (200 µL) and CH_3CN (800 µL) into the reactor. The aqueous solution was carefully evaporated to dryness *in vacuo*. The precursor **22** (5 mg, 7.5 µmol, 1 eq) in CH_3CN (1 mL) was added to the reactor and the mixture was stirred at 110 °C for 30 min. Then, the solvent was evaporated *in vacuo*. TFA (1 mL) and water (100 µL) were added. The reaction mixture was stirred at 40 °C for 5 min. The solvent was evaporated *in vacuo*. MeOH (1 mL) was added to the reactor and the solution was transferred into a flask outside the synthesizer. The solution was concentrated to a volume of 500 µL and diluted with water (500 µL). Purification was performed by semipreparative radio-HPLC

(Method C2). The product fraction of **[^{18}F]19** (t_R = 37.6 min) was evaporated to dryness *in vacuo* and the residue was dissolved in water:EtOH (1 mL , 9:1). Pyrazole **[^{18}F]19** was obtained with a rcy of 22 ± 9 % (d. c., *n* = 9) and a rcp >99 % (t_R (analytical radio-HPLC, Method D) = 11.7 min) and a A_m in the range of 3 - 68 GBq/µmol in 161 ± 15 min.

Determination of log$D_{7.4}$–values of radiobabeled compounds

The lipophilicity of **[^{18}F]4**, **[^{18}F]9** and **[^{18}F]19** were determined following the procedure described by Prante *et al.*.[65] An amount of 29-232 kBq radiolabelled compound in PBS buffer (10 µL, pH 7.4) was added to PBS buffer (490 µL, pH 7.4) and octan-1-ol (500 µL). The two-phase mixture was shaken for 3 min on a vortexer at room temperature and centrifuged (3000 rpm) for 5 min. The octanol layer (400 µL) was collected carefully and added to a new tube with PBS buffer (400 µL, pH 7.4). The two phase mixture was shaken again for 10 min and centrifuged for 5 min. Three samples were prepared and 100 µL of both phases were measured in a γ-counter (Wallac Wizard, PERKIN-ELMER LIFE-SCIENCE). The partition coefficient was determined by dividing cpm(octanol) by cpm(PBS) and indicated as log$D_{7.4}$.

***In vitro* serum stability in human and mouse serum**

The stability of the radiolabeled compounds **[^{18}F]4**, **[^{18}F]9** and **[^{18}F]19** in human and murine serum was measured after incubation at 37 °C for 90 min. An aliquot of formulated solution in PBS-buffer (40 µL, approximately 10 MBq) was added to a tube with blood serum (200 µL) and the mixture was shaken at 37 °C. After 10, 20, 30, 60 and 90 min an aliquot (20 µL) was taken out of the tube and added to cooled MeOH:CH_2Cl_2 solution (1:1 , 100 µL). The sample was analyzed by analytical radio-HPLC (Method D) after centrifugation for 5 min.

***In vitro* biotransformation in mouse liver microsome suspensions**

For the *in vitro* identification of metabolites previous methods were adapted.[60,61] For the determination of exact masses and for conducting MS/MS experiments, an LC system was coupled with a qTOF.

The following HPLC-DAD (THERMOFISHER) system was used: pump: DGP-3600RS; DAD-detector: DAD-3000RS (λ = 230 and 250 nm); precolumn: Security guard TM cartridge C_{18} 4.0 µm, 4.0 mm x 2.0 mm; column: Phenomenex Synergi Hydro RP 2.6 µm, 50 mm x 2.1 mm,; column oven: TCC-3000RS, 30 °C; autosampler: WPS-3000RS; solvent rack: SRD 3600; HPLC-MS Method E (**12a** and **12b**): pump 1: solvent A: water:acetonitrile:HCO_2H 900:100:1; solvent B: acetonitrile:water:HCO_2H 900:100:1; flow rate: 0.3 mL/min (0.0 – 7.0 min, 9.9 – 10.0 min) and 0.4 mL/ min (7.0 – 9.9 min); gradient elution: (A%): 0.0 min: 100%, 0.0 – 5.0 min: gradient from 100% to 0%, 5.0 – 6.5 min: 0%, 6.5 – 7.0 min: gradient from 0% to 100%, 7.0 – 10.0 min: 100%. HPLC-MS Method F (**19**): pump 1: solvent A: water:acetonitrile:HCO_2H 900:100:1; solvent B: acetonitrile:water:HCO_2H 900:100:1; flow rate: 0.1 mL/min (0.0 – 3.0 min, 17.9 – 18.0 min) and 0.4 mL/ min (3.0 – 17.9 min); gradient elution: (A%): 0.0 – 3.1 min: 100%, 3.1 – 12.0 min: gradient from 100% to 0%, 12.0 – 14.5 min: 0%, 14.5 – 15.0 min: gradient from 0% to 100%, 15.0 – 18.0 min: 100%; pump 2: solvent C: water:HCO_2H 1000:1; flow rate: 0.3 mL/min (0.0 – 3.0 min, 17.9 – 18.0 min) and 0.0 mL/ min (3.0 – 17.9 min); elution: (C%): 0.0 – 18.0 min: 100%. As volumes >10 µL were injected, online dilution was used. Therefore, a second pump with an aqueous solvent was added to the method to dilute the solvent of the first pump in a ratio of 1:4.

The LC system was coupled with a microOTOF-Q II (BRUKER DALTONICS). The ESI-qTOF was operated in positive and negative ion polarity in the full scan mode (*m/z* = 70 – 700) with the

following settings: capillary voltage: 4500 V; end plate offset: -500 V; collision cell RF: 300.0 Vpp; nebulizer: 2.0 bar; dry heater: 200 °C; dry gas: 9.0 L/min.

In case of MS/MS experiments the isolation window of the first quadrupole was set to 10 *m/z* units. The collision energy of the second quadrupole was 35 eV. Data handling and control of the system were realized with the software DataAnalysis and Hystar from BRUKER DALTONICS . The calibration of the TOF spectra was achieved by injection of $LiHCO_2$ (isopropanol:bidist. water 1:1, 10 mM) via a 20 µL sample loop within each LC run at 2.0 – 2.2 min.

Experimental procedure: DMSO stock solution (1.0 µL, 10 mM) of the compound **12a**, **12b** or **19** was added to PBS (pH 7.4, 23 µL, 0.1 M), $MgCl_2$ solution (50 µL, 50 mM), NADPH solution (50 µL, 2 mg/mL in PBS), UDPGA solution (50 µL, 2 mg/mL in PBS) and mice liver microsome suspension (26 µL, 7.8 mg protein/mL). In case of the incubation without UDPGA 50 µL PBS was added instead. The suspension was mixed vigorously and shaken for 90 min or 120 min at 37 °C (900 rpm). The incubation was stopped by addition of icecold acetonitrile/methanol (1:1, 400 µL). The Eppendorf cups were cooled down to 0 °C for 10 min using a water/ice bath. The precipitated proteins were separated via centrifugation (15 min, 16000 rpm, 4 °C) and the supernatant was analyzed by the above described LC-MS method. With the same procedure, the empty value (without stock solution), the blank value (without cofactors) and in the case of **19** a buffer sample (199 µL PBS and 1 µL DMSO stock solution) were prepared. To detect possible impurities in the stock solution a positive control (599 µL solvent and 1 µL DMSO stock solution) was prepared for **19** additionally.

Table 2: Identification of **36** (t_R = 9.9 min) via fragmentation.

m/z obs.	*m/z* calcd.	formula

458.1387	458.1380	$C_{22}H_{24}N_3O_6S^+$
449.1191	449.1177	$C_{21}H_{22}FN_2O_6S^+$
430.1051	430.1067	$C_{20}H_{20}N_3O_6S^+$
345.0702	345.0704	$C_{17}H_{14}FN_2O_3S^+$
279.0926	279.0928	$C_{17}H_{12}FN_2O^+$

***In vitro* binding to human serum albumin**

In vitro HSA binding of triazoles **4** and **9** and pyrazoles **17** and **19** was investigated by HPAC using an analytical HPLC column coated with HSA, as already described.[64]

***In vivo* Biodistribution studies**

Animals. For biodistribution studies male C57BL/6 mice (24-30 g body weight) were used at the age of 12-15 weeks and housed under specific pathogen-free conditions.

All experiments performed in the study were in accordance with the german law on the care and use of laboratory animals and approved by the local authorizing agency of North Rhine-Westphalia.

Small animal PET scanning. For PET experiments mice were anesthetized by 3 % isoflurane in air. Tracers **[^{18}F]4**, **[^{18}F]9** and **[^{18}F]19** were intravenously injected into the mice as bolus (100 µL) by injection pump controlled saline flush (300 µL/min) via the tail vein and subsequent PET scanning was performed. PET experiments were performed using a small animal scanner (32module quadHIDAC, Oxford Positron Systems Ltd., Oxford, UK). The scanner has a high resolution (0.7 mm full width at half maximum) with uniform spatial resolution (<1 mm) over a large cylindrical field (165 mm diameter, 280 mm axial length). With an iterative reconstruction

algorithm data were acquired for 120 min and reconstructed into dynamic time frames. The scanning bed was transferred to the CT scanner (Inveon, Siemens Medical Solutions, U.S.) and a CT acquisition was performed for each mouse with a spatial resolution of 80 µm. Image data sets were co-registered with extrinsic markers attached to the multimodal scanning bed and the in-house developed image analysis software MEDgical. In CT data sets the three-dimensional volumes of interest (VOIs) were defined over the relevant organs, transferred to the co-registered PET data and analyzed quantitatively. By dividing counts per milliliter in the VOI by total counts in the mouse multiplied by 100 (% ID/mL) regional uptake was calculated as percentage of injected dose by dividing counts per milliliter in the VOI.

ASSOCIATED CONTENT

Supporting Information. The Supporting Information is available free of charge on the ACS Publications website at DOI:

Experimental procedures and analytical data for the compounds **11a-b**, **12a-b**, **13**, **14**, **16**, **17**, *ent*-**18**, *ent*-**19** and **20-31**, ^{1}H- and ^{13}C-NMR spectra of compounds **4**, **9** and **19**, experimental procedure for the measurement of *in vitro* binding to serum albumin.

Molecular formula strings.

AUTHOR INFORMATION

Corresponding Author. *Tel.: +49-251-8344713; Fax: +49-251-8347363; E-mail: stefan.wagner@ukmuenster.de

ORCID. Stefan Wagner: 0000-0001-6207-3617

ACKNOWLEDGEMENTS

The authors thank Christine Bätza, Stefanie Bouma, Claudia Essmann, Sven Fatum, Sandra Höppner, Marlena Kattenbeck, Sarah Köster, Nina Kreienkamp, Sandra Laumann, Philipp Pingen, Roman Priebe, Katrin Reckmann and Dirk Reinhardt for technical support and the staff members of the Organic Chemistry Institute and Department of Pharmaceutical and Medicinal Chemistry, University of Münster, Germany, for spectroscopic and analytical investigations. This work was supported by the Deutsche Forschungsgemeinschaft (DFG), Collaborative Research Center 656 (Molecular Cardiovascular Imaging Projects A02, Z05 and C06) and the and the Interdisciplinary Centre of Clinical Research (IZKF core unit PIX), Münster Germany.

ABBREVIATIONS USED

A_m, molar activity; BSA, bovine serum albumin; DAST, Diethylaminosulfur trifluoride; d. c., decay corrected; DME, 1,2-Dimethoxyethane; DMEDA, *N,N'*-Dimethylethylenediamine; DMF, *N,N*-Dimethylformamide; DMSO, Dimethyl sulfoxide; EDC, 1-Ethyl-3-(3-dimethylaminopropyl)carbodiimide; HOBT, 1-Hydroxybenzotriazole; HSA, human serum albumin; ID, injected dose; MMP, matrix metalloproteinase; MMPI, matrix metalloproteinase inhibitor; MOPS, 3-Morpholinopropanesulfonic acid; NMM, *N*-Methylmorpholine; PBS, phosphate buffered saline; PET, positron emission tomography; SPECT, single photon emission computed tomography; rcp, radiochemical purity; rcy, radiochemical yield; rt, room temperature; TFA, Trifluoroacetic acid; THP, 2-Tetrahydropyranyl; TLC, thin layer chromatography; Ts, Tosyl; VOI, volume of interest.

REFERENCES

1. Maskos, K.; Bode, W. Structural basis of matrix metalloproteinases and tissue inhibitors of metalloproteinases. *Mol. Biotechnol.* **2003**, *25*, 241-266.
2. Mittal, R.; Patel, A. P.; Debs, L. H.; Nguyen, D.; Patel, K.; Grati, M.; Mittal, J.; Yan, D.; Chapagain, P.; Liu, X. Z. Intricate functions of matrix metalloproteinases in physiological and pathological conditions. *J. Cell Physiol.* **2016**, *231*, 2599-2621.
3. Tokito, A.; Jougasaki, M. Matrix metalloproteinases in non-neoplastic disorders. *Int. J. Mol. Sci.* **2016**, *17*, 1178.
4. Jabłońska-Trypuć, A.; Matejczyk, M.; Rosochacki, S. Matrix metalloproteinases (MMPs), the main extracellular matrix (ECM) enzymes in collagen degradation, as a target for anticancer drugs. *J. Enzyme Inhib. Med. Chem.* **2016**, *31*(sup1), 177-183.
5. Cathcart, J.; Pulkoski-Gross, A.; Cao, J. Targeting matrix metalloproteinases in cancer: Bringing new life to old ideas. *Genes Dis.* **2015**, *2*, 26-34.
6. Amin, M.; Pushpakumar, S.; Muradashvili, N.; Kundu, S; Tyagi, S. C.; Sen, U. Regulation and involvement of matrix metalloproteinases in vascular diseases. *Front. Biosci. (Landmark Ed.)* **2016**, *21*, 89-118.
7. Newby, A. C. Metalloproteinases promote plaque rupture and myocardial infarction: A persuasive concept waiting for clinical translation. *Matrix Biol.* **2015**, *44-46*, 157-166.
8. De Stefano, M. E.; Herrero, M. T. The multifaceted role of metalloproteinases in physiological and pathological conditions in embryonic and adult brains. *Prog. Neurobiol.* **2017**, *155*, 36-56.
9. Sun, H. B. Mechanical loading, cartilage degradation, and arthritis. *Ann. N. Y. Acad. Sci.* **2010**, *1211*, 37-50.

10. Houghton, A. M. Matrix metalloproteinases in destructive lung disease. *Matrix Biol.* **2015**, *44-46*, 167-174.

11. Matusiak, N.; van Waarde, A.; Bischoff, R.; Oltenfreiter, R.; van de Wiele, C.; Dierckx, R.A.; Elsinga, P. H. Probes for non-invasive matrix metalloproteinase-targeted imaging with PET and SPECT. *Curr. Pharm. Des.* **2013**, *19*, 4647-4672.

12. MacPherson, L. J.; Bayburt, E. K.; Capparelli, M. P.; Carroll, B. J.; Goldstein, R.: Justice, M. R.; Zhu, L.; Hu, S.; Melton, R. A.; Fryer, L.; Goldberg, R. L.; Doughty, J. R.; Spirito, S.; Blancuzzi, V.; Wilson, D.; O'Byrne, E. M.; Ganu, V.; Parker, D. T. Discovery of CGS 27023A, a non-peptidic, potent, and orally active stromelysin inhibitor that blocks cartilage degradation in rabbits. *J. Med. Chem.* **1997**, *40*, 2525-1532.

13. Scozzafava, A.; Supuran, C. T. Carbonic anhydrase and matrix metalloproteinase inhibitors: Sulfonylated amino acid hydroxamates with MMP inhibitory properties act as efficient inhibitors of CA isozymes I, II, and IV, and *N*-hydroxysulfonamides inhibit both these zinc enzymes. *J. Med. Chem.* **2000**, *43*, 3677-3687.

14. Kopka, K.; Breyholz, H. J.; Wagner, S.; Law, M. P.; Riemann, B.; Schröer, S.; Trub, M.; Guilbert, B.; Levkau, B.; Schober, O.; Schäfers, M. Synthesis and preliminary biological evaluation of new radioiodinated MMP inhibitors for imaging MMP activity in vivo. *Nucl. Med. Biol.* **2004**, *31*, 257-267.

15. Schäfers, M.; Riemann, B.; Kopka, K.; Breyholz, H. J.; Wagner, S.; Schäfers, K. P.; Law, M. P.; Schober, O.; Levkau B. Scintigraphic imaging of matrix metalloproteinase activity in the arterial wall in vivo. *Circulation* **2004**, *109*, 2554-2559.

16. Breyholz, H. J.; Wagner, S.; Levkau, B.; Schober, O.; Schäfers, M.; Kopka, K. A ^{18}F-radiolabelled analogue of CGS 27023A for assessment of matrix-metalloproteinase activity in vivo. *Q. J. Nucl. Med. Mol. Imaging* **2007**, *51*, 24-32.

17. Wagner, S.; Breyholz, H. J.; Law, M. P.; Faust, A.; Höltke, C.; Schröer, S.; Haufe, G.; Levkau, B.; Schober, O.; Schäfers, M.; Kopka, K. Novel fluorinated derivatives of the broad-spectrum MMP inhibitors *N*-Hydroxy-2(*R*)-[[(4-methoxyphenyl)sulfonyl](benzyl)- and (3-picolyl)-amino]-3-methyl-butanamide as potential tools for the molecular imaging of activated MMPs with PET. *J. Med. Chem.* **2007**, *50*, 5752-5764.

18. Wagner, S.; Breyholz, H. J.; Höltke, C.; Faust, A.; Schober, O.; Schäfers, M.; Kopka, K. A new ^{18}F-labelled derivative of the MMP inhibitor CGS 27023A for PET: Radiosynthesis and initial small-animal PET studies. *Appl. Radiat. Isot.* **2009**, *67*, 606-610.

19. Wagner S, Faust A, Breyholz HJ, Schober O, Schäfers M, Kopka K. The MMP inhibitor (*R*)-2-(*N*-benzyl-4-(2-[^{18}F]fluoroethoxy)phenylsulphonamido)-*N*-hydroxy-3-methylbutanamide: Improved precursor synthesis and fully automated radiosynthesis. *Appl. Radiat. Isot.* **2011**, *69*, 862–868.

20. Gerwien, H.; Hermann, S.; Zhang, X.; Korpos, E.; Song, J.; Kopka, K.; Faust, A.; Wenning, C.; Gross, C. C.; Honold, L.; Melzer, N.; Opdenakker, G.; Wiendl, H.; Schäfers, M.; Sorokin, L. Imaging matrix metalloproteinase activity in multiple sclerosis as a specific marker of leukocyte penetration of the blood-brain barrier. *Sci. Transl. Med.* **2016**, *8*, 364ra15.

21. Hugenberg, V.; Breyholz, H. J.; Riemann, B.; Hermann, S.; Schober, O.; Schäfers, M.; Gangadharmath, U.; Mocharla, V.; Kolb, H.; Walsh, J.; Zhang, W.; Kopka, K.; Wagner,

S. A new class of highly potent matrix metalloproteinase inhibitors based on triazole-substituted hydroxamates: (Radio)synthesis, *in vitro* and first *in vivo* evaluation. *J. Med. Chem.* **2012**, *55*, 4714-4727.

22. Hugenberg, V.; Riemann, B.; Hermann, S.; Schober, O.; Schäfers, M.; Szardenings, K.; Lebedev, A.; Gangadharmath, U.; Kolb, H.; Walsh, J.; Zhang, W.; Kopka, K.; Wagner, S. Inverse 1,2,3-triazole-1-yl-ethyl substituted hydroxamates as highly potent matrix metalloproteinase inhibitors: (Radio)synthesis, in vitro and first in vivo evaluation. *J. Med. Chem.* **2013**, *56*, 6858–6870.
23. Hugenberg, V.; Hermann, S.; Galla, F.; Schäfers, M.; Wünsch, B.; Gangadharmath, U.; Mocharla, V.; Kolb, H.; Lebedev, A.; Walsh, J.; Zhang, W.; Kopka, K.; Wagner, S. Radiolabeled hydroxamate-based matrix metalloproteinase inhibitors: How chemical modifications affect pharmacokinetics and metabolic stability. *Nucl. Med. Biol.* **2016**, *43*, 424-437.
24. Grams, F.; Brandstetter, H.; D'Alo, S.; Geppert, D.; Krell, H.W.; Leinert, H.; Livi, V.; Menta, E.; Oliva, A.; Zimmermann, G. Pyrimidine-2,4,6-triones: A new effective and selective class of matrix metalloproteinase inhibitors. *Biol. Chem.* **2001**, *382*, 1277-1285.
25. Breyholz, H. J.; Schäfers, M.; Wagner, S.; Höltke, C.; Faust, A.; Rabeneck, H.; Levkau, B.; Schober, O.; Kopka, K. C-5-Disubstituted barbiturates as potential molecular probes for noninvasive matrix metalloproteinase imaging. *J. Med. Chem.* **2005**, *48*, 3400-3409.
26. Breyholz, H. J.; Kopka, K.; Schäfers, M.; Wagner, S. Syntheses of radioiodinated pyrimidine-2,4,6-triones as potential agents for non-invasive imaging of matrix metalloproteinases. *Pharmaceuticals* **2017**, *10*, 49.

27. Breyholz, H. J.; Wagner, S.; Faust, A.; Riemann, B.; Hermann, S.; Schober, O.; Schäfers, M.; Kopka, K. Radiofluorinated pyrimidine-2,4,6-triones as molecular probes for non-invasive MMP-targeted imaging. *ChemMedChem* **2010**, *5*, 777-789.

28. Schrigten, D.; Breyholz, H. J.; Wagner, S.; Hermann, S.; Schober, O.; Schäfers, M.; Haufe, G.; Kopka, K. A new generation of radiofluorinated pyrimidine-2,4,6-triones as MMP-targeted radiotracers for positron emission tomography. *J. Med. Chem.* **2012**, *55*, 223-232.

29. Vazquez, N.; Missault, S.; Vangestel, C.; Deleye, S.; Thomae, D.; Van der Veken, P.; Augustyns, K.; Staelens, S.; Dedeurwaerdere, S.; Wyffels, L. Evaluation of [^{18}F]BR420 and [^{18}F]BR351 as radiotracers for MMP-9 imaging in colorectal cancer. *J. Labelled Comp. Radiopharm.* **2017**, *60*, 69-79.

30. Kalinin, D. V.; Wagner, S.; Riemann, B.; Hermann, S.; Schmidt, F.; Becker-Pauly, C.; Rose-John, S.; Schäfers, M.; Holl, R. Novel potent proline-based metalloproteinase inhibitors: Design, (radio)synthesis and first *in vivo* evaluation as radiotracers for positron emission tomography, *J. Med. Chem.* **2016**, *59*, 9541-5959.

31. Hugenberg, V.; Wagner, S.; Kopka, K.; Schäfers, M.; Schuit, R.; Windhorst, A. D.; Hermann, S. Radiolabeled selective MMP-13 inhibitors: (Radio)syntheses, *in vitro* and first *in vivo* evaluations. *J. Med. Chem.* **2017**, *60*, 307-321.

32. Withrow, J.; Murphy, C.; Liu, Y.; Hunter, M.; Fulzele, S.; Hamrick, M. W. Extracellular vesicles in the pathogenesis of rheumatoid arthritis and osteoarthritis. *Arthritis Res. Ther.* **2016**, *18*, 286.

33. Churg, A.; Zhou, S.; Wright, J. L. Series "matrix metalloproteinases in lung health and disease": Matrix metalloproteinases in COPD. *Eur. Respir. J.* **2012**, *39*, 197-209.

34. Chaudhuri, R.; McSharry, C.; Brady, J.; Donnelly, I.; Grierson, C.; McGuinness, S.; Jolly, L.; Weir, C.J.; Messow, C. M.; Spears, M.; Miele, G.; Nocka, K.; Crowther, D.; Thompson, J.; Brannigan, M.; Lafferty, J.; Sproule, M.; Macnee, W.; Connell, M.; Murchison, J. T.; Shepherd, M.C.; Feuerstein, G.; Miller, D. K.; Thomson, N. C. Sputum matrix metalloproteinase-12 in patients with chronic obstructive pulmonary disease and asthma: Relationship to disease severity. *J Allergy Clin. Immunol.* **2012**, *129*, 655-663.

35. Takahashi, S.; Ishii, M.; Namkoong, H.; Hegab, A. E.; Asami, T.; Yagi, K.; Sasaki, M.; Haraguchi, M.; Sato, M.; Kameyama, N.; Asakura, T.; Suzuki, S.; Tasaka, S.; Iwata, S.; Hasegawa, N.; Betsuyaku, T. Pneumococcal infection aggravates elastase-induced emphysema via matrix metalloproteinase 12 overexpression. *J. Infect. Dis.* **2016**, *213*, 1018-1030.

36. Chelluboina, B.; Nalamolu, K. R.; Klopfenstein, J. D.; Pinson, D. M.; Wang, D. Z.; Vemuganti, R.; Veeravalli, K. K. MMP-12, a Promising therapeutic target for neurological diseases. *Mol. Neurobiol.* **2017**, *55*, 1405-1409.

37. Wang, P.; Chen S. H.; Hung, W. C.; Paul, C.; Zhu, F.; Guan, P. P.; Huso, D. L.; Kontrogianni-Konstantopoulos, A.; Konstantopoulos, K. Fluid shear promotes chondrosarcoma cell invasion by activating matrix metalloproteinase 12 via IGF-2 and VEGF signaling pathways. *Oncogene* **2015**, *34*, 4558-4569.

38. Ng, K. T.; Qi, X.; Kong, K. L.; Cheung, B. Y.; Lo, C. M.; Poon, R. T.; Fan, S. T.; Man, K. Overexpression of matrix metalloproteinase-12 (MMP-12) correlates with poor prognosis of hepatocellular carcinoma. *Eur. J. Cancer* **2011**, *47*, 2299-2305.

39. Morgan, A. R.; Rerkasem, K.; Gallagher, P. J.; Zhang, B.; Morris, G. E.; Calder, P. C.; Grimble, R. F.; Eriksson, P.; McPheat, W. L.; Shearman, C. P.; Ye, S. Differences in

matrix metalloproteinase-1 and matrix metalloproteinase-12 transcript levels among carotid atherosclerotic plaques with different histopathological characteristics. *Stroke* **2004**, *35*, 1310-1315.

40. Yu, Y.; Koike, T.; Kitajima, S.; Liu, E.; Morimoto, M.; Shiomi, M.; Hatakeyama, K.; Asada, Y.; Wang, K. Y.; Sasaguri, Y.; Watanabe, T.; Fan, J. Temporal and quantitative analysis of expression of metalloproteinases (MMPs) and their endogenous inhibitors in atherosclerotic lesions. *Histol. Histopathol.* **2008**, *12*, 1503-1516.
41. Johnson, J. L.; Devel, L.; Czarny, B.; George, S. J.; Jackson, C. L.; Rogakos, V.; Beau, F.; Yiotakis, A.; Newby, A. C.; Dive, V. A selective matrix metalloproteinase-12 inhibitor retards atherosclerotic plaque development in apolipoprotein E-knockout mice. *Arterioscler. Thromb. Vasc. Biol.* **2011**, *31*, 528-535.
42. Newby, A. C. Proteinases and plaque rupture: unblocking the road to translation. *Curr. Opin. Lipidol.* **2014**, *25*, 358-366.
43. Eckelman, W. C. The application of receptor theory to receptor-binding and enzyme-binding oncologic radiopharmaceuticals. *Nucl. Med. Biol.* **1994**, *21*, 759-769.
44. Sprague, J. E.; Li, W. P.; Liang, K.; Achilefu, S.; Anderson, C. J. In vitro and in vivo investigation of matrix metalloproteinase expression in metastatic tumor models. *Nucl. Med. Biol.* **2006**, *33*, 227-237.
45. Casalini, F.; Fugazza, L.; Esposito, G.; Cabella, C.; Brioschi, C.; Cordaro, A.; D'Angeli, L.; Bartoli, A.; Filannino, A. M.; Gringeri, C. V.; Longo, D. L.; Muzio, V.; Nuti, E.; Orlandini, E.; Figlia, G.; Quattrini, A.; Tei, L.; Digilio, G.; Rossello, A.; Maiocchi, A. Synthesis and preliminary evaluation in tumor bearing mice of new ^{18}F-labeled

arylsulfone matrix metalloproteinase inhibitors as tracers for positron emission tomography. *J. Med. Chem.* **2013**, *56*, 2676-2689.

46. Koppisetti, R.K.; Fulcher, Y.G.; Jurkevich, A.; Prior, S. H.; Xu, J.; Lenoir, M.; Overduin, M.; Van Doren, S. R. Ambidextrous binding of cell and membrane bilayers by soluble matrix metalloproteinase-12. *Nat. Commun.* **2014**, *21*, 5:5552.
47. Marchant, D. J.; Bellac, C. L.; Moraes, T. J.; Wadsworth, S. J.; Dufour, A.; Butler, G. S.; Bilawchuk, L. M.; Hendry, R. G.; Robertson, A. G.; Cheung, C. T.; Ng, J.; Ang, L.; Luo, Z.; Heilbron, K.; Norris, M. J.; Duan, W.; Bucyk, T.; Karpov, A.; Devel, L.; Georgiadis, D.; Hegele, R. G.; Luo, H.; Granville, D. J.; Dive, V.; McManus, B. M.; Overall, C. M. A new transcriptional role for matrix metalloproteinase-12 in antiviral immunity. *Nat. Med.* **2014**, *20*, 493-502.
48. Kondo, N.; Temma, T.; Aita, K.; Shimochi, S.; Koshino, K.; Senda, M.; Iida, H. Development of matrix metalloproteinase-targeted probes for lung inflammation detection with positron emission tomography. *Sci. Rep.* **2018**, *8*, 1347.
49. Toczek, J.; Ye, Y.; Gona, K.; Kim, H. Y.; Han, J.; Razavian, M.; Golestani, R.; Zhang, J.; Wu, T. L.; Jung, J. J.; Sadeghi, M. M. Preclinical evaluation of RYM1, a matrix metalloproteinase-targeted tracer for imaging aneurysm. *J. Nucl. Med.* **2017**, *58*, 1318-1323.
50. Wu, Y.; Li, J.; Wu, J.; Morgan, P.; Xu, X.; Rancati, F.; Vallese, S.; Raveglia, L.; Hotchandani, R.; Fuller, N.; Bard, J.; Cunningham, K.; Fish, S.; Krykbaev, R.; Tam, S.; Goldman, S. J.; Williams, C.; Mansour, T. S.; Saiah, E.; Sypek, J.; Li, W. Discovery of potent and selective matrix metalloprotease 12 inhibitors for the potential treatment of

chronic obstructive pulmonary disease (COPD). *Bioorg. Med. Chem. Lett.* **2012**, *22*, 138-143.

51. Li, W.; Li, J., Wu, J.; Tam, S.; Mansour, T.; Sypek, J.; Joseph, P.; Mcfayden, I.; Hotchandani, R.; Wu, J. Preparation of tricyclic compounds as matrix metalloproteinase inhibitors. *From PCT Int. Appl.* **2008**, *13*, 2008137816.
52. Harrison, T. J.; Dake, G. R. Pt(II) or Ag(I) salt catalyzed cycloisomerizations and tandem cycloadditions forming functionalized azacyclic arrays. *Org. Lett.* **2004**, *6*, 5023–5026.
53. Glaser, M.; Årstad, E. "Click Labeling" with 2-[^{18}F]fluoroethylazide for positron emission tomography. *Bioconjugate Chem.* **2007**, *18*, 989–993.
54. Huang, W.; Meng, Q.; Suzuki, K.; Nagase, H.; Brew, K. Mutational study of the amino-terminal domain of human tissue inhibitor of metalloproteinases-I (Timp-1) locates an inhibitory region for matrix metalloproteinases. *J. Biol. Chem.* **1997**, *272*, 22086–22091.
55. Galla, F.; Bourgeois, C.; Lehmkuhl, K.; Schepmann, D.; Soeberdt, M.; Lotts, T.; Abels, C.; Ständer, S.; Wünsch, B. Effects of polar κ receptor agonists designed for the periphery on ATP-induced Ca^{2+} release from keratinocytes. *MedChemComm.* **2016**, *7*, 317–326.
56. Fabre, B.; Ramos, A.; de Pascual-Teresa, B. Targeting matrix metalloproteinases: Exploring the dynamics of the S1' pocket in the design of selective, small molecule inhibitors. *J. Med. Chem.* **2014**, *57*, 10205-10219.
57. Li, W.; Li, J.; Wu, Y.; Wu, J.; Hotchandani, R.; Cunningham, K.; McFadyen, I.; Bard, J.; Morgan, P.; Schlerman, F.; Xu, X.; Tam, S.; Goldman, S. J.; Williams, C.; Sypek, J.; Mansour, T. S. A selective matrix metalloprotease 12 inhibitor for potential treatment of chronic obstructive pulmonary disease (COPD): Discovery of (*S*)-2-(8-

(methoxycarbonylamino)dibenzo[b,d]furan-3-sulfonamido)-3-methylbutanoic acid (MMP408). *J. Med. Chem.* **2009**, *52*, 1799-1802.

58. Li, W.; Li, J.; Wu, Y.; Rancati, F.; Vallese, S.; Raveglia, L.; Wu, J.; Hotchandani, R.; Fuller, N.; Cunningham, K.; Morgan, P.; Fish, S.; Krykbaev, R.; Xu, X.; Tam, S.; Goldman, S. J.; Abraham, W.; Williams, C.; Sypek, J.; Mansour, T. S. Identification of an orally efficacious matrix metalloprotease 12 inhibitor for potential treatment of asthma. *J. Med. Chem.* **2009**, *52*, 5408-5419.
59. Rouanet-Mehouas, C.; Czarny, B.; Beau, F.; Cassar-Lajeunesse, E.; Stura, E. A.; Dive, V.; Devel, L. Zinc-metalloproteinase inhibitors: Evaluation of the complex role played by the zinc-binding group on potency and selectivity. *J. Med. Chem.* **2017**, *60*, 403-414.
60. Ortmeyer, C. P.; Haufe, G.; Schwegmann, K.; Hermann, S.; Schäfers, M.; Börgel, F.; Wünsch, B.; Wagner, S.; Hugenberg, V. Synthesis and evaluation of a [^{18}F]BODIPY-labeled caspase-inhibitor. *Bioorg. Med. Chem.* **2017**, *25*, 2167-2176.
61. Heimann, D.; Börgel, F.; de Vries, H.; Bachmann, K.; Rose, V.; Frehland, B.; Schepmann, D.; Heitmann, L. H.; Wünsch, B. Optimization of pharmacokinetic properties by modification of a carbazole-based cannabinoid receptor subtype 2 (CB_2) ligand. *Eur. J. Med. Chem*. **2018**, *143*, 1436-1447.
62. Zhang, F.; Xue, J.; Shao, J.; Jia, L. Compilation of 222 drugs' plasma protein binding data and guidance for study designs. *Drug Discov. Today* **2012**, *17*, 475–485.
63. Colombo, S.; Buclin, T,; Décosterd, L. A.; Telenti, A.; Furrer, H.; Lee, B. L.; Biollaz, J.; Eap, C. B. Orosomucoid (alpha1-acid glycoprotein) plasma concentration and genetic variants: Effects on human immunodeficiency virus protease inhibitor clearance and cellular accumulation. *Clin. Pharmacol. Ther.* **2006**, *80*, 307–318.

64. Galla, F. Analytical tools for the determination of pharmacokinetic parameters *in vitro*: Case study with matrix metalloproteinase inhibitors, *PhD thesis*, **2016**, Münster, Germany.

65. Prante, O.; Hocke, C.; Gmeiner, P.; Kuwert, T. Tissue distribution of radioiodinated FAUC113: Assessment of a pyrazole [1,5-*a*]pyridine-based dopamine D4 receptor radioligand candidate. *Nuklearmedizin* **2006**, *45*, 41–48.

Table of Contents graphic.